

Transport theory for interacting electrons connected to reservoirs

Akira Oguri

*Department of Material Science, Osaka City University,
Sumiyoshi-ku, Osaka 558-8585, Japan*

March 13, 2018

Abstract

We describe microscopic theory for the quantum transport through finite interacting systems connected to noninteracting leads. It can be applied to small systems such as quantum dots, quantum wires, atomic chain, molecule, and so forth. The Keldysh formalism is introduced to study the nonlinear current-voltage characteristics, and general properties of the nonequilibrium Green's functions are provided. We apply the formulated to an out-of-equilibrium Anderson model that has been used widely for the Kondo effect in quantum dots. In the linear-response regime the Kubo formalism still has an advantage, because it relates the transport coefficients directly to the correlation functions defined with respect to the thermal equilibrium, and it has no ambiguities about a profile of the inner electric field. We introduce a many-body transmission coefficient, by which the dc conductance can be expressed in a Landauer-type form, quite generally. We also discuss transport properties of the Tomonaga-Luttinger liquid, which has also been an active field of research in this decade.

Contents

1	Introduction	3
2	Keldysh formalism for quantum transport	4
2.1	Thermal equilibrium	4
2.2	Statistical weight for nonequilibrium steady states	5
2.3	Perturbation expansion along the Keldysh contour	7
2.4	Nonequilibrium Green's function	9
2.5	Green's function for the initial state	11
2.6	Nonequilibrium current for noninteracting electrons	11
3	Out-of-equilibrium Anderson model	13
3.1	Green's function for the Anderson impurity	13
3.2	Properties of the Green's functions at $eV = 0$	16
3.3	Current through the Anderson impurity	17
3.4	Perturbation expansion with respect to \mathcal{H}_C^U	18
3.5	Fermi-liquid behavior at low bias voltages	20
4	Transport theory based on Kubo formalism	22
4.1	Many-body transmission coefficient $\mathcal{T}(\epsilon)$	23
4.2	Current Conservation and Ward identity	27
4.3	Lehmann representation for $\mathcal{T}(\epsilon)$	29
4.4	Application to a Hubbard chain connected to leads	31
5	Tomonaga-Luttinger Model	34
5.1	Spin-less fermions in one dimension	34
5.2	Two conservation laws	37
5.3	Charge and current correlation functions	38
5.4	Boson representation of the Hamiltonian	41

1 Introduction

Quantum transport through finite interacting-electron systems has been studied extensively in this decade. For instance, the Coulomb blockade and various effects named after Kondo, Aharonov-Bohm, Fano, Josephson, etc. in quantum dot systems have been a very active field of research. Furthermore, the realization of non-Fermi liquid systems such as the Tomonaga-Luttinger liquid in quantum wires and multi-channel Kondo behavior in some novel systems have also been investigated by a number theorists.

To study transport properties of correlated electron systems, theoretical approaches that can treat correctly both the interaction and quantum interference effects are required. The Keldysh Green's function approach is one of such methods [1, 2, 3, 4, 5, 6, 7, 8, 9]. Specifically, the formulation for the nonlinear current-voltage profile by Caroli *et al* has been applied widely to the quantum transport phenomena. In this report, we describe the outline of the Keldysh formalism in Sec. 2, and then apply it to a single Anderson impurity, which is a standard model of quantum dots in the Kondo regime in Sec. 3.

When a finite sample is connected to reservoirs that can be approximated by free-electron systems with continuous energy spectrums, the low-energy eigenstates of whole the system including the attached reservoirs are determined coherently. Thus, to understand the low-temperature properties, the information about the low-lying energy states of the whole system is required. The local Fermi-liquid theory [10, 11], which was originally introduced for the Kondo systems [12], is also applicable to the transport properties in wide classes of the interacting-electron systems at low temperatures. In Sec. 4, we reformulate the transport theory for the interacting systems connected to noninteracting leads based on the Kubo formalism. The dc conductance can be written in a Landauer-type form with a many-body transmission coefficient determined by a three-point correlation function. We also provide a brief introduction to Tomonaga-Luttinger model in Sec. 5 to take a quick look at the transport properties of a typical interacting-electron system in one dimension.

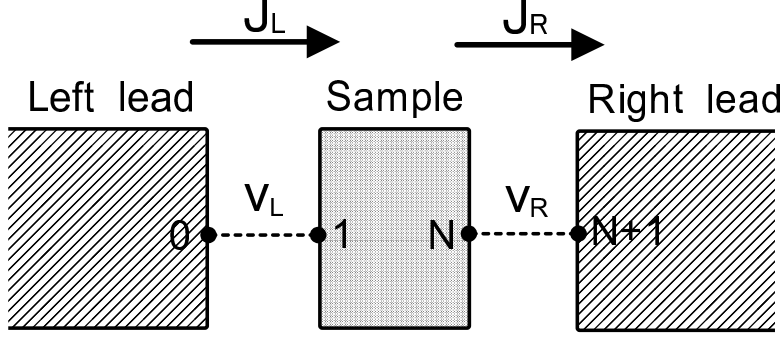


Figure 1: Schematic picture of the system.

2 Keldysh formalism for quantum transport

2.1 Thermal equilibrium

We start with a system that consists of three regions: a finite central region (C) and two reservoirs on the left (L) and the right (R). The central region consists of N resonant levels, and the interaction $U_{j_4 j_3; j_2 j_1}$ is switched on only for the electrons in this region. We assume that each of the reservoirs is infinitely large and has a continuous energy spectrum. The central region and reservoirs are connected with the mixing matrix elements v_L and v_R , as illustrated in Fig. 1. The complete Hamiltonian is given by

$$\mathcal{H}_{\text{tot}}^{\text{eq}} = \mathcal{H}_L + \mathcal{H}_R + \mathcal{H}_C^0 + \mathcal{H}_C^U + \mathcal{H}_{\text{mix}}. \quad (1)$$

$$\mathcal{H}_L = - \sum_{ij \in L} t_{ij}^L c_{i\sigma}^\dagger c_{j\sigma}, \quad \mathcal{H}_R = - \sum_{ij \in R} t_{ij}^R c_{i\sigma}^\dagger c_{j\sigma}, \quad (2)$$

$$\mathcal{H}_C^0 = - \sum_{ij \in C} t_{ij}^C c_{i\sigma}^\dagger c_{j\sigma}, \quad \mathcal{H}_C^U = \frac{1}{2} \sum_{\substack{\{j\} \in C \\ \sigma\sigma'}} U_{j_4 j_3; j_2 j_1} c_{j_4\sigma}^\dagger c_{j_3\sigma'}^\dagger c_{j_2\sigma'} c_{j_1\sigma}, \quad (3)$$

$$\mathcal{H}_{\text{mix}} = - \sum_{\sigma} v_L \left[c_{0\sigma}^\dagger c_{-1\sigma} + \text{H.c.} \right] - \sum_{\sigma} v_R \left[c_{N+1\sigma}^\dagger c_{N\sigma} + \text{H.c.} \right]. \quad (4)$$

Here, $c_{j\sigma}^\dagger$ ($c_{j\sigma}$) creates (destroys) an electron with spin σ at site j , and μ is the chemical potential. Also, t_{ij}^L , t_{ij}^R , and t_{ij}^C are the intra-region hopping matrix elements in each of the three regions L , R , and C , respectively. The labels $1, 2, \dots, N$ are assigned to the sites in the central region. Specifically,

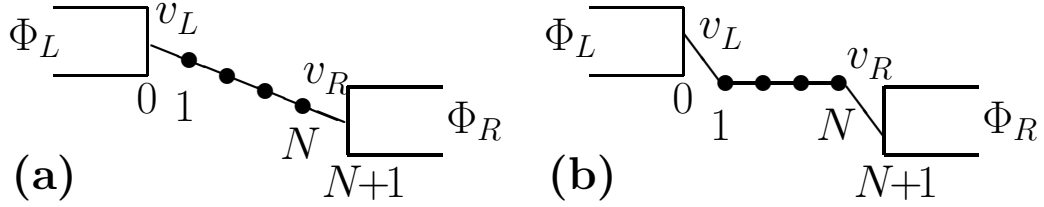


Figure 2: Examples for the profile of the electrostatic potential $\Phi_C(i)$ for (a) an insulating sample, and (b) a metal sample, where $eV = \Phi_L - \Phi_R$.

the label 1 (N) is assigned to the site at the interface on the left (right), and the label 0 ($N + 1$) is assigned to the site at the reservoir-side of the left (right) interface. We will be using units $\hbar = 1$ unless otherwise noted.

The density matrix for the equilibrium state ρ_{eq} is given by

$$\rho_{\text{eq}} = e^{-\beta\{\mathcal{H}_{\text{tot}}^{\text{eq}} - \mu(N_L + N_C + N_R)\}} / \text{Tr} e^{-\beta\{\mathcal{H}_{\text{tot}}^{\text{eq}} - \mu(N_L + N_C + N_R)\}}, \quad (5)$$

$$N_L = \sum_{i \in L, \sigma} c_{i\sigma}^\dagger c_{i\sigma}, \quad N_C = \sum_{i \in C, \sigma} c_{i\sigma}^\dagger c_{i\sigma}, \quad N_R = \sum_{i \in R, \sigma} c_{i\sigma}^\dagger c_{i\sigma}. \quad (6)$$

Therefore, the Hamiltonian $\mathcal{H}_{\text{tot}}^{\text{eq}}$ and a single chemical potential μ determine the statistical weight in thermal equilibrium.

2.2 Statistical weight for nonequilibrium steady states

When the voltage V is applied, the contribution of the electrostatic potential has to be included into $\mathcal{H}_{\text{tot}}^{\text{eq}}$, as

$$\mathcal{H}_{\text{tot}} = \mathcal{H}_{\text{tot}}^{\text{eq}} + \mathcal{V}_{\text{ext}}, \quad (7)$$

$$\mathcal{V}_{\text{ext}} = \Phi_L N_L + \Phi_R N_R + \sum_{i \in C, \sigma} \Phi_C(i). \quad (8)$$

Here Φ_L and Φ_R are the potentials for the lead at L and R , respectively, and the applied bias voltage corresponds to $eV \equiv \Phi_L - \Phi_R$. To determine the potential profile in the central region $\Phi_C(i)$, the energy of the electric field should also be included into the Hamiltonian eq. (2), and it should be determined self-consistently. However for simplicity, we assume that $\Phi_C(i)$ is a given function. In Fig. 2, two typical profiles are illustrated. For an insulating sample, there must be a finite electric field in the central region

and the potential shows approximately a linear i -dependence as that in the panel (a). In an opposite case, for a metallic sample, the electric field vanishes in the central region, and the potential profile will become the one as shown in the panel (b). Realistic situations seem to be in between these two extreme cases.

In contrast to the thermal equilibrium, one cannot write down the density matrix that describes the nonequilibrium statistical weight simply by using a single chemical potential,

$$\rho \neq e^{-\beta\{\mathcal{H}_{\text{tot}}-\mu(N_L+N_C+N_R)\}} / \text{Tr} e^{-\beta\{\mathcal{H}_{\text{tot}}-\mu(N_L+N_C+N_R)\}}, \quad (9)$$

because this statistical weight describes the situation after the electrons have already been redistributed to gain the electrostatic potential energy. One possible statistical weight that describes a nonequilibrium steady state was introduced by Caroli *et al* [4].

In the formulation of Caroli *et al*, the coupling to the leads \mathcal{H}_{mix} and the interaction \mathcal{H}_C^U in the sample region are switched on adiabatically by separating the total Hamiltonian in the form

$$\mathcal{H}_{\text{tot}}(t) = \mathcal{H}_1 + \mathcal{H}_2(t), \quad (10)$$

$$\mathcal{H}_1 = \mathcal{H}_{1;L} + \mathcal{H}_{1;C} + \mathcal{H}_{1;R}, \quad (11)$$

$$\mathcal{H}_{1;L} = \mathcal{H}_L + \Phi_L N_L, \quad \mathcal{H}_{1;R} = \mathcal{H}_R + \Phi_R N_R, \quad (12)$$

$$\mathcal{H}_{1;C} = \mathcal{H}_C^0 + \sum_{i \in C, \sigma} \Phi_C(i) c_{i\sigma}^\dagger c_{i\sigma}, \quad (13)$$

$$\mathcal{H}_2(t) = \left[\mathcal{H}_{\text{mix}} + \mathcal{H}_C^U \right] e^{-\delta|t|}. \quad (14)$$

Here, $\delta = 0^+$ is a positive infinitesimal. Because \mathcal{H}_1 has a quadratic form, it is possible to use the Wick theorem in the perturbation expansion with respect to \mathcal{H}_2 . At $t = -\infty$ the two reservoirs and the impurity are isolated, so that the different chemical potentials μ_L , μ_R , and μ_C can be introduced into the three regions in the initial condition. The time evolution of the density matrix is determined by the equation

$$\frac{\partial}{\partial t} \rho(t) = -i \left[\mathcal{H}_{\text{tot}}(t), \rho(t) \right]. \quad (15)$$

The formal solution of this equation can be obtained, by using the interaction representation $\tilde{\rho}(t) = e^{i\mathcal{H}_1 t} \rho(t) e^{-i\mathcal{H}_1 t}$ and $\tilde{\mathcal{H}}_2(t) = e^{i\mathcal{H}_1 t} \mathcal{H}_2(t) e^{-i\mathcal{H}_1 t}$, as

$$\tilde{\rho}(t) = U(t, t_0) \tilde{\rho}(t_0) U(t_0, t), \quad (16)$$

$$U(t, t_0) = \text{T exp} \left[-i \int_{t_0}^t dt' \widetilde{\mathcal{H}}_2(t') \right], \quad (17)$$

$$U(t_0, t) = \widetilde{\text{T}} \text{ exp} \left[i \int_{t_0}^t dt' \widetilde{\mathcal{H}}_2(t') \right]. \quad (18)$$

Here, T denotes the operator for the chronological time order, and $\widetilde{\text{T}}$ is the anti-time-ordering operator. Note that eq. (18) is the Hermite conjugatae of eq. (17). Caroli *et al* have assumed that the initial condition at $t_0 \rightarrow -\infty$ is given by

$$\widetilde{\rho}(-\infty) = \frac{e^{-\beta\{\mathcal{H}_{1,L}-\mu_L N_L\}} e^{-\beta\{\mathcal{H}_{1,C}-\mu_C N_C\}} e^{-\beta\{\mathcal{H}_{1,R}-\mu_R N_R\}}}{\text{Tr} \left[e^{-\beta\{\mathcal{H}_{1,L}-\mu_L N_L\}} e^{-\beta\{\mathcal{H}_{1,C}-\mu_C N_C\}} e^{-\beta\{\mathcal{H}_{1,R}-\mu_R N_R\}} \right]}. \quad (19)$$

Namely, at $t_0 \rightarrow -\infty$, each system is in a thermal equilibrium state with the chemical potential $\mu_{L,R,C}$. Here $\mu_L - \mu_R = \Phi_L - \Phi_R = eV$.

2.3 Perturbation expansion along the Keldysh contour

The perturbed part $\widetilde{\mathcal{H}}_2(t)$ is switched fully on at $t = 0$. Therefore the expectation value of physical quantities are defined with respect to the density matrix at $t = 0$,

$$\begin{aligned} \langle \mathcal{O} \rangle &\equiv \text{Tr} [\rho(0) \mathcal{O}_S] \\ &= \text{Tr} [\widetilde{\rho}(0) \mathcal{O}_S] = \text{Tr} [\widetilde{\rho}(-\infty) U(-\infty, 0) \mathcal{O}_S U(0, -\infty)], \end{aligned} \quad (20)$$

where \mathcal{O}_S is a Schrödinger operator, and $[\rho(0), \mathcal{H}_{\text{tot}}(0)] = 0$ for the stationary states. Equation (20) can be rewritten by using a property of the time-evolution operator, $U(-\infty, 0) = U(-\infty, +\infty) U(+\infty, 0)$, as

$$\langle \mathcal{O} \rangle = \langle U(-\infty, +\infty) U(+\infty, 0) \mathcal{O}_S U(0, -\infty) \rangle_0, \quad (21)$$

where $\langle \cdots \rangle_0 \equiv \text{Tr} [\widetilde{\rho}(-\infty) \cdots]$. The stream of the time in eq. (21) can be mapped onto a loop shown in Fig. 3: starting from $t = -\infty$, observing a quantity \mathcal{O} at $t = 0$, then proceeding to $t = +\infty$, and then going back to $t = -\infty$. In the case of the usual $T = 0$ Green's function with respect to the equilibrium ground state, the wavefunction at $t = +\infty$ is essentially the same with the one at $t = -\infty$ apart from a phase factor if the initial state has no degeneracy [13]. Thus, eq. (21) can be decoupled at the time $t = +\infty$. However, this simplification does not take place in the nonequilibrium case

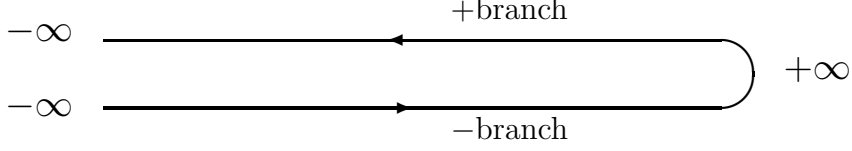


Figure 3: The Keldysh contour for the time evolution.

of the initial condition eq. (19), Therefore, one has to treat the time loop including the way back to $t \rightarrow -\infty$.

The time-dependent expectation value is defined by using the Heisenberg operator $\mathcal{O}_H(t)$, and is written in the form

$$\begin{aligned}
\langle \mathcal{O}(t) \rangle &\equiv \text{Tr} [\rho(0) \mathcal{O}_H(t)] \\
&= \langle U(-\infty, +\infty) U(+\infty, t) \tilde{\mathcal{O}}(t) U(t, -\infty) \rangle_0 \\
&= \langle U(-\infty, +\infty) \{ \text{T} U(+\infty, -\infty) \tilde{\mathcal{O}}(t) \} \rangle_0 \\
&= \langle \text{T}_c U_c \tilde{\mathcal{O}}(t^-) \rangle_0.
\end{aligned} \tag{22}$$

Here, the relation among the Schrödinger \mathcal{O}_S , interaction $\tilde{\mathcal{O}}(t)$, and Heisenberg $\mathcal{O}_H(t)$ representations are given by

$$\tilde{\mathcal{O}}(t) = e^{i\mathcal{H}_1 t} \mathcal{O}_S e^{-i\mathcal{H}_1 t}, \quad \mathcal{O}_H(t) = U(0, t) \tilde{\mathcal{O}}(t) U(t, 0). \tag{23}$$

In eq. (22), T_c and U_c express the time order and time evolution along the Keldysh contour, respectively, and t^- denotes the time in the $-$ branch in Fig. 3.

The perturbation expansion with respect to \mathcal{H}_2 can be carried out by substituting eqs. (17) and (18), respectively, into $U(+\infty, -\infty)$ and $U(-\infty, +\infty)$ in eq. (22), as

$$\begin{aligned}
\langle \mathcal{O}(t) \rangle &= \sum_{n=0}^{\infty} \sum_{m=0}^{\infty} \frac{i^n}{n!} \frac{(-i)^m}{m!} \int_{-\infty}^{+\infty} dt'_1 \cdots dt'_n \int_{-\infty}^{+\infty} dt_1 \cdots dt_m \\
&\quad \times \langle \{ \tilde{\text{T}} \tilde{\mathcal{H}}_2(t'_1) \cdots \tilde{\mathcal{H}}_2(t'_n) \} \{ \text{T} \tilde{\mathcal{H}}_2(t_1) \cdots \tilde{\mathcal{H}}_2(t_m) \tilde{\mathcal{O}}(t) \} \rangle_0.
\end{aligned} \tag{24}$$

The Wick's theorem is applicable to the average $\langle \cdots \rangle_0$ because \mathcal{H}_1 has a bilinear form. However, because $U(+\infty, -\infty)$ gives a factor $(-i)^m$ for the m -th order terms while $U(-\infty, +\infty)$ gives a factor $(+i)^n$ for the n -th order terms, four types of the Green's functions are necessary to distinguish the contributions from these two branches.

Lifshitz-Pitaevskii	G^{--}	G^{++}	G^{+-}	G^{-+}
Alternative notation	G_c	\tilde{G}_c	$G^>$	$G^<$

Table 1: Correspondence between two standard notations.

2.4 Nonequilibrium Green's function

We now introduce the four types of the Green's functions, which are required in the Feynman-diagrammatic approach to the perturbation expansion along the time loop,

$$\begin{aligned}
G_{ij}^{--}(t_1, t_2) &\equiv -i \langle T c_{i\sigma}(t_1) c_{j\sigma}^\dagger(t_2) \rangle \\
&= -i \langle T_C U_c \tilde{c}_{i\sigma}(t_1^-) \tilde{c}_{j\sigma}^\dagger(t_2^-) \rangle_0, \tag{25}
\end{aligned}$$

$$\begin{aligned}
G_{ij}^{++}(t_1, t_2) &\equiv -i \langle \tilde{T} c_{i\sigma}(t_1) c_{j\sigma}^\dagger(t_2) \rangle \\
&= -i \langle T_C U_c \tilde{c}_{i\sigma}(t_1^+) \tilde{c}_{j\sigma}^\dagger(t_2^+) \rangle_0, \tag{26}
\end{aligned}$$

$$\begin{aligned}
G_{ij}^{+-}(t_1, t_2) &\equiv -i \langle c_{i\sigma}(t_1) c_{j\sigma}^\dagger(t_2) \rangle \\
&= -i \langle T_C U_c \tilde{c}_{i\sigma}(t_1^+) \tilde{c}_{j\sigma}^\dagger(t_2^-) \rangle_0, \tag{27}
\end{aligned}$$

$$\begin{aligned}
G_{ij}^{-+}(t_1, t_2) &\equiv i \langle c_{j\sigma}^\dagger(t_2) c_{i\sigma}(t_1) \rangle \\
&= -i \langle T_C U_c \tilde{c}_{i\sigma}(t_1^-) \tilde{c}_{j\sigma}^\dagger(t_2^+) \rangle_0. \tag{28}
\end{aligned}$$

Here $c_{i\sigma}(t_1)$ and $c_{j\sigma}^\dagger(t_2)$ are Heisenberg operators. $t^{+,-}$ denotes the time + or -branch in Fig. 3. For these Green's functions, there is another notation used widely in literatures, and the relation between that and the present one by Lifshitz-Pitaevskii [5] is summarized in Table 1.

Based on the Feynman-diagrammatic approach, the Dyson equation can be expressed in a 2×2 matrix form;

$$\mathbf{G}_{ij}(\omega) = \mathbf{g}_{ij}(\omega) + \sum_{lm} \mathbf{g}_{il}(\omega) \boldsymbol{\Sigma}_{lm}(\omega) \mathbf{G}_{mj}(\omega), \tag{29}$$

$$\mathbf{G}_{ij} = \begin{bmatrix} G_{ij}^{--} & G_{ij}^{-+} \\ G_{ij}^{+-} & G_{ij}^{++} \end{bmatrix}, \quad \boldsymbol{\Sigma}_{lm} = \begin{bmatrix} \Sigma_{lm}^{--} & \Sigma_{lm}^{-+} \\ \Sigma_{lm}^{+-} & \Sigma_{lm}^{++} \end{bmatrix}. \tag{30}$$

Here, \mathbf{g}_{ij} is the Green's function determined by the unperturbed Hamiltonian \mathcal{H}_1 and density matrix $\tilde{\rho}(-\infty)$ for the initial isolated system. The Fourier

transform has been carried out for stationary states,

$$G(t_1, t_2) = \int_{-\infty}^{\infty} \frac{d\omega}{2\pi} G(\omega) e^{-i\omega(t_1-t_2)}. \quad (31)$$

For instance, in the noninteracting case $\mathcal{H}_C^U = 0$, the self-energy correction is caused only by the couplings between the sample and reservoirs \mathcal{H}_{mix} ,

$$\begin{aligned} \Sigma_{ij}^0 &= -v_L (\delta_{i,-1}\delta_{j,0} + \delta_{i,0}\delta_{j,-1}) \begin{bmatrix} 1 & 0 \\ 0 & -1 \end{bmatrix} \\ &\quad -v_R (\delta_{i,N}\delta_{m,N+1} + \delta_{i,N+1}\delta_{m,N}) \begin{bmatrix} 1 & 0 \\ 0 & -1 \end{bmatrix}. \end{aligned} \quad (32)$$

Note that the four types Green's functions are not independent,

$$G^{--} + G^{++} = G^{+-} + G^{-+}, \quad \Sigma^{--} + \Sigma^{++} = -\Sigma^{-+} - \Sigma^{+-}. \quad (33)$$

Thus, the Dyson equation eq. (29) can be expressed in terms of three independent quantities by carrying out a Unitary transformation $\mathbf{P}^{-1}\mathbf{G}\mathbf{P}$;

$$\mathbf{P} = \frac{1}{\sqrt{2}} \begin{bmatrix} 1 & 1 \\ -1 & 1 \end{bmatrix}, \quad (34)$$

$$\begin{bmatrix} 0 & G_{ij}^a \\ G_{ij}^r & F_{ij} \end{bmatrix} = \begin{bmatrix} 0 & g_{ij}^a \\ g_{ij}^r & F_{ij}^0 \end{bmatrix} + \sum_{lm} \begin{bmatrix} 0 & g_{il}^a \\ g_{il}^r & F_{il}^0 \end{bmatrix} \begin{bmatrix} \Omega_{lm} & \Sigma_{lm}^r \\ \Sigma_{lm}^a & 0 \end{bmatrix} \begin{bmatrix} 0 & G_{mj}^a \\ G_{mj}^r & F_{mj} \end{bmatrix}. \quad (35)$$

Here, G^r and G^a are the retarded and advanced Green's functions, respectively,

$$G^r = G^{--} - G^{-+}, \quad G^a = G^{--} - G^{+-}, \quad F = G^{--} + G^{++}, \quad (36)$$

$$\Sigma^r = \Sigma^{--} + \Sigma^{-+}, \quad \Sigma^a = \Sigma^{--} + \Sigma^{+-}, \quad \Omega = \Sigma^{--} + \Sigma^{++}. \quad (37)$$

The function F and Ω link closely to a nonequilibrium distribution. Alternatively, the original four Green's functions can be expressed with these three functions, as

$$G^{--} = [F + (G^r + G^a)]/2, \quad G^{++} = [F - (G^r + G^a)]/2, \quad (38)$$

$$G^{-+} = [F - (G^r - G^a)]/2, \quad G^{+-} = [F + (G^r - G^a)]/2. \quad (39)$$

Similarly, the four self-energies are written in terms of Σ^r , Σ^a and Ω ,

$$\Sigma^{--} = [\Omega + (\Sigma^r + \Sigma^a)]/2, \quad \Sigma^{++} = [\Omega - (\Sigma^r + \Sigma^a)]/2, \quad (40)$$

$$\Sigma^{-+} = -[\Omega - (\Sigma^r - \Sigma^a)]/2, \quad \Sigma^{+-} = -[\Omega + (\Sigma^r - \Sigma^a)]/2. \quad (41)$$

The Dyson equation for the three functions are deduced from eq. (35)

$$G^r = g^r + g^r \Sigma^r G^r, \quad G^a = g^a + g^a \Sigma^a G^a, \quad (42)$$

$$F = F^0 + F^0 \Sigma^a G^a + g^r \Sigma^r F + g^r \Omega G^a. \quad (43)$$

Here, we have suppressed the subscripts for simplicity, and these equations should be understood symbolically. Eq. (43) can be solved formally by using eq. (42), as

$$\begin{aligned} F &= [1 - g^r \Sigma^r]^{-1} F^0 [1 + \Sigma^a G^a] + [1 - g^r \Sigma^r]^{-1} g^r \Omega G^a, \\ &= G^r \{g^r\}^{-1} F^0 \{g^a\}^{-1} G^a + G^r \Omega G^a. \end{aligned} \quad (44)$$

2.5 Green's function for the initial state

The unperturbed Green's function g_{ij} is determined by \mathcal{H}_1 and the initial density matrix $\tilde{\rho}(-\infty)$. Initially at $t \rightarrow \infty$, the three regions are isolated and noninteracting. Therefore, $g_{ij;\nu}$ for $\nu = L, R, C$ is given by

$$g_{ij;\nu}^r(\omega) = \sum_n \frac{\phi_{n;\nu}(i)\phi_{n;\nu}^*(j)}{\omega - \epsilon_{n;\nu} + i\delta}, \quad g_{ij;\nu}^a(\omega) = \sum_n \frac{\phi_{n;\nu}(i)\phi_{n;\nu}^*(j)}{\omega - \epsilon_{n;\nu} - i\delta}, \quad (45)$$

$$F_{ij;\nu}^0(\omega) = [1 - 2f_\nu(\omega)] [g_{ij;\nu}^r(\omega) - g_{ij;\nu}^a(\omega)]. \quad (46)$$

Here, $\epsilon_{n;\nu}$ and $\phi_{n;\nu}(i)$ are the one-particle eigenvalue and eigenstate of $\mathcal{H}_{1;\nu}$. The information about the statistical distribution is contained in the function $F_{ij;\nu}^0$ via $f_\nu(\omega) = f(\omega - \mu_\nu)$, where $f(\epsilon) = [e^{\beta\epsilon} + 1]^{-1}$. In the system we are considering, each of the reservoirs ($\nu = L, R$) has a continuous energy spectrum, and the isolated sample ($\nu = C$) has a discrete energy spectrum. Thus, the full Green's function becomes to depend only on μ_L and μ_R , and does not depend on μ_C [14]. This is because the contribution of F^0 to the corresponding full one F arises in a sandwiched form $\{g^r\}^{-1} F^0 \{g^a\}^{-1}$ as described in eq. (44). Thus, the singular contributions of δ functions in $F^0 \propto [g^r - g^a]$ of the sample region are canceled out by the zero points of the inverse Green's functions in both sides, to yield $\{g^r\}^{-1} F^0 \{g^a\}^{-1} = 0$ for $\nu = C$.

2.6 Nonequilibrium current for noninteracting electrons

The nonequilibrium average of the charge and current can be deduced from the Green's functions. For instance, by using eqs. (28) and (31), an equal-

time correlation function can be written in the form

$$\langle c_{i\sigma}^\dagger c_{j\sigma} \rangle = -iG_{ji}^{-+}(0,0) = -i \int_{-\infty}^{\infty} \frac{d\omega}{2\pi} G_{ji}^{-+}(\omega). \quad (47)$$

Therefore, the current flowing from the left lead to the sample is given by

$$J_L = iev_L \sum_{\sigma} \left[c_{1\sigma}^\dagger c_{0\sigma} - c_{0\sigma}^\dagger c_{1\sigma} \right], \quad (48)$$

$$\langle J_L \rangle = 2ev_L \int_{-\infty}^{\infty} \frac{d\omega}{2\pi} \left[G_{01}^{-+}(\omega) - G_{10}^{-+}(\omega) \right]. \quad (49)$$

The expectation value for the current flowing from the sample to right lead, J_R , can also be written in a similar form. In the noninteracting case $\mathcal{H}_C^U = 0$, eq. (49) can be rewritten in terms of retarded and advanced Green's functions which link the two different interfaces of the sample [4];

$$\langle J \rangle = \frac{2e}{h} \int_{-\infty}^{\infty} d\omega [f_L(\omega) - f_R(\omega)] \mathcal{T}_0(\omega), \quad (50)$$

$$\mathcal{T}_0(\omega) = 4 \Gamma_L(\omega) G_{1N}^a(\omega) \Gamma_R(\omega) G_{N1}^r(\omega), \quad (51)$$

$$\Gamma_L(\omega) = -\text{Im} \left[v_L^2 g_{00}^r(\omega) \right], \quad \Gamma_R(\omega) = -\text{Im} \left[v_R^2 g_{N+1N+1}^r(\omega) \right]. \quad (52)$$

Note that $\langle J_L \rangle = \langle J_R \rangle (\equiv \langle J \rangle)$ in steady states. The outline of the derivation are provided in Sec. 3.3 for a single Anderson impurity. Equation (51) implies that the current is determined by the electrons with the energy $\mu_R \lesssim \omega \lesssim \mu_L$ at low temperatures, where $\mu_L - \mu_R = eV$.

For interacting electron systems, the nonequilibrium current can not generally be written in the form of eq. (50). It does only in a particular case where the connection of the two leads and the sample has a special symmetry described by a relation $\mathbf{\Gamma}^L(\epsilon) = \lambda \mathbf{\Gamma}^R(\epsilon)$ in the notation used in Ref. [15]. In the interacting case, the imaginary part of the self-energy caused by the inelastic scattering becomes finite. It links with the contributions of the vertex corrections, and the formulation becomes somewhat complicated. Nevertheless, in the linear-response regime, the dc conductance for interacting electrons can be expressed in a Landauer-type form quite generally [16, 17, 18] even in the case without the special symmetry mentioned above [19]. Specifically, at zero temperature $T = 0$, the imaginary part of the self-energy and vertex corrections for the current become zero at the Fermi energy $\omega = 0$, and the transmission probability can be written in the form of eq. (51) with the interacting Green's functions. We discuss the details of these points in Sec. 4.

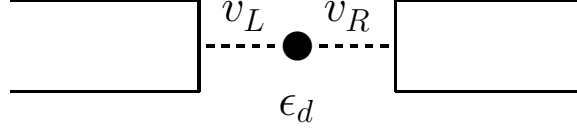


Figure 4: Anderson impurity connected to two leads

3 Out-of-equilibrium Anderson model

We now apply the Keldysh formalism to a single Anderson impurity connected to two leads as illustrated in Fig. 3. It corresponds to the $N = 1$ case of the Hamiltonian eq. (1), and has been widely used as a model for quantum dots. For convenience, we change the label for the sites: the new one for the impurity site is given by $0 \Rightarrow d$, and that for the interfaces at the left and right leads are $0 \Rightarrow L$ and $N + 1 \Rightarrow R$, respectively.

3.1 Green's function for the Anderson impurity

The self-energy in the interacting case can be classified into two parts.

$$\Sigma_{ij}(\omega) = \Sigma_{ij}^0(\omega) + \Sigma_U(\omega) \delta_{i,d} \delta_{j,d}. \quad (53)$$

Here, Σ_{ij}^0 corresponds to the one defined in eq. (32), which represents the effects purely due to the mixing with reservoirs and sample. The remaining part Σ_U contains the contributions of the onsite Coulomb interaction U . Substituting the self-energy eq. (53) into the Dyson equation (29), we obtain a set of equations for the impurity Green's function,

$$\begin{aligned} \mathbf{G}_{dd}(\omega) &= \mathbf{g}_{dd}(\omega) + \mathbf{g}_{dd}(\omega) \Sigma_U(\omega) \mathbf{G}_{dd}(\omega) \\ &\quad - v_L \mathbf{g}_{dd}(\omega) \tau_3 \mathbf{G}_{Ld}(\omega) - v_R \mathbf{g}_{dd}(\omega) \tau_3 \mathbf{G}_{Rd}(\omega), \end{aligned} \quad (54)$$

$$\mathbf{G}_{Ld}(\omega) = -v_L \mathbf{g}_L(\omega) \tau_3 \mathbf{G}_{dd}(\omega), \quad (55)$$

$$\mathbf{G}_{Rd}(\omega) = -v_R \mathbf{g}_R(\omega) \tau_3 \mathbf{G}_{dd}(\omega). \quad (56)$$

where g_L and g_R are the Green's function at the interfaces at left and right, respectively. The explicit form of the unperturbed Green's function at the

impurity site is given by $\{\mathbf{g}_{dd}(\omega)\}^{-1} = (\omega - \epsilon_d) \boldsymbol{\tau}_3$ with one of the Pauli matrices $\boldsymbol{\tau}_3$. Substituting eqs. (55) and (56) into eq. (54), we obtain

$$\mathbf{G}_{dd}(\omega) = \mathbf{g}_{dd}(\omega) + \mathbf{g}_{dd}(\omega) [\boldsymbol{\sigma}(\omega) + \boldsymbol{\Sigma}_U(\omega)] \mathbf{G}_{dd}(\omega), \quad (57)$$

$$\boldsymbol{\sigma}(\omega) = v_L^2 \boldsymbol{\tau}_3 \mathbf{g}_L(\omega) \boldsymbol{\tau}_3 + v_R^2 \boldsymbol{\tau}_3 \mathbf{g}_R(\omega) \boldsymbol{\tau}_3. \quad (58)$$

Therefore,

$$\{\mathbf{G}_{dd}(\omega)\}^{-1} = \{\mathbf{G}_{dd}^{(0)}(\omega)\}^{-1} - \boldsymbol{\Sigma}_U(\omega), \quad (59)$$

$$\{\mathbf{G}_{dd}^{(0)}(\omega)\}^{-1} = \{\mathbf{g}_{dd}(\omega)\}^{-1} - \boldsymbol{\sigma}(\omega). \quad (60)$$

Here $\mathbf{G}_{dd}^{(0)}(\omega)$ is the Green's function for the noninteracting case. Furthermore, an alternatively form of the Dyson equation $G = g + G \Sigma g$ yields

$$\mathbf{G}_{dL}(\omega) = -v_L \mathbf{G}_{dd}(\omega) \boldsymbol{\tau}_3 \mathbf{g}_L(\omega) \quad (61)$$

$$\mathbf{G}_{dR}(\omega) = -v_R \mathbf{G}_{dd}(\omega) \boldsymbol{\tau}_3 \mathbf{g}_R(\omega). \quad (62)$$

Thus, the inter-site Green's functions can be deduced from $\mathbf{G}_{dd}(\omega)$ by using eqs. (55)–(56) and (61)–(62).

The voltage-dependence arises via the unperturbed Green's functions for the leads at $\nu = L$ and R ,

$$\mathbf{g}_\nu(\omega) = \mathbf{P} \begin{bmatrix} 0 & g_\nu^a(\omega) \\ g_\nu^r(\omega) & F_\nu^0(\omega) \end{bmatrix} \mathbf{P}^{-1}, \quad (63)$$

$$\begin{aligned} F_\nu^0(\omega) &= [1 - 2f_\nu(\omega)][g_\nu^r(\omega) - g_\nu^a(\omega)], \\ &= -2i[1 - 2f_\nu(\omega)]\Gamma_\nu(\omega)/v_\nu^2, \end{aligned} \quad (64)$$

where $\Gamma_\nu(\omega) \equiv -v_\nu^2 \text{Im}[g_\nu^r(\omega)]$. The pure mixing part of the self energy $\boldsymbol{\sigma}(\omega)$ can be calculated from eqs. (58) and (63),

$$\boldsymbol{\sigma}(\omega) = \mathbf{P} \begin{bmatrix} \Omega^{(0)}(\omega) & \sigma^r(\omega) \\ \sigma^a(\omega) & 0 \end{bmatrix} \mathbf{P}^{-1}, \quad (65)$$

$$\Omega^{(0)}(\omega) = v_L^2 F_L^0(\omega) + v_R^2 F_R^0(\omega), \quad (66)$$

$$\sigma^r(\omega) = v_L^2 g_L^r(\omega) + v_R^2 g_R^r(\omega), \quad (67)$$

and $\sigma^a(\omega) = \{\sigma^r(\omega)\}^*$. Then the noninteracting Green's function $\mathbf{G}_{dd}^{(0)}(\omega)$ can be determined via eq. (60),

$$G_{dd}^{(0) --}(\omega) = [1 - f_{\text{eff}}(\omega)] G_{dd}^{(0)r}(\omega) + f_{\text{eff}}(\omega) G_{dd}^{(0)a}(\omega), \quad (68)$$

$$G_{dd}^{(0) ++}(\omega) = -f_{\text{eff}}(\omega) G_{dd}^{(0)r}(\omega) - [1 - f_{\text{eff}}(\omega)] G_{dd}^{(0)a}(\omega), \quad (69)$$

$$G_{dd}^{(0) -+}(\omega) = -f_{\text{eff}}(\omega) [G_{dd}^{(0)r}(\omega) - G_{dd}^{(0)a}(\omega)], \quad (70)$$

$$G_{dd}^{(0) +-}(\omega) = [1 - f_{\text{eff}}(\omega)] [G_{dd}^{(0)r}(\omega) - G_{dd}^{(0)a}(\omega)], \quad (71)$$

where

$$f_{\text{eff}}(\omega) = \frac{f_L(\omega) \Gamma_L + f_R(\omega) \Gamma_R}{\Gamma_L + \Gamma_R}, \quad (72)$$

$$G_{dd}^{(0)r}(\omega) = \frac{1}{\omega - \epsilon_d - \sigma^r(\omega)}, \quad (73)$$

and $G_{dd}^{(0)a}(\omega) = \{G_{dd}^{(0)r}(\omega)\}^*$. Thus, the effects of the bias voltage arise through the distribution function $f_{\text{eff}}(\omega)$.

The full Green's function for the impurity site can be expressed, using eqs. (42)–(44) and (64)–(66), as

$$G_{dd}^r(\omega) = \frac{1}{\omega - \epsilon_d - \sigma^r(\omega) - \Sigma_U^r(\omega)}, \quad (74)$$

$$F_{dd}(\omega) = G_{dd}^r(\omega) [\Omega^{(0)}(\omega) + \Omega_U(\omega)] G_{dd}^a(\omega), \quad (75)$$

where $G_{dd}^a(\omega) = \{G_{dd}^r(\omega)\}^*$. Note that $\Omega_U(\omega) = -\Sigma_U^{-+}(\omega) - \Sigma_U^{+-}(\omega)$ and $F_{dd}(\omega)$ are pure imaginary. The four elements of $\mathbf{G}_{dd}(\omega)$ can be written, using eqs. (38)–(39) and (74)–(75), as

$$G_{dd}^{--}(\omega) = [1 - \tilde{f}_{\text{eff}}(\omega)] G_{dd}^r(\omega) + \tilde{f}_{\text{eff}}(\omega) G_{dd}^a(\omega), \quad (76)$$

$$G_{dd}^{++}(\omega) = -\tilde{f}_{\text{eff}}(\omega) G_{dd}^r(\omega) - [1 - \tilde{f}_{\text{eff}}(\omega)] G_{dd}^a(\omega), \quad (77)$$

$$G_{dd}^{-+}(\omega) = -\tilde{f}_{\text{eff}}(\omega) [G_{dd}^r(\omega) - G_{dd}^a(\omega)], \quad (78)$$

$$G_{dd}^{+-}(\omega) = [1 - \tilde{f}_{\text{eff}}(\omega)] [G_{dd}^r(\omega) - G_{dd}^a(\omega)], \quad (79)$$

where $G_{dd}^{++}(\omega) = -\{G_{dd}^{--}(\omega)\}^*$, and $\tilde{f}_{\text{eff}}(\omega)$ is a correlated distribution defined by

$$\tilde{f}_{\text{eff}}(\omega) = \frac{f_L(\omega) \Gamma_L + f_R(\omega) \Gamma_R - \frac{1}{2i} \Sigma_U^{-+}(\omega)}{\Gamma_L + \Gamma_R - \text{Im} \Sigma_U^r(\omega)}. \quad (80)$$

With this distribution function, the number of the electrons in the impurity site can be written in the form

$$\langle n_d \rangle = 2 \int d\omega \tilde{f}_{\text{eff}}(\omega) \left(-\frac{1}{\pi} \right) \text{Im} G_{dd}^r(\omega). \quad (81)$$

In the equilibrium case $\mu \equiv \mu_L = \mu_R$, both $\tilde{f}_{\text{eff}}(\omega)$ and $f_{\text{eff}}(\omega)$ coincide with the Fermi function $f(\omega)$, because of the property eq. (84).

3.2 Properties of the Green's functions at $eV = 0$

We summarize here the properties of the Keldysh Green's function in the limit of the zero-bias voltage $eV = 0$, at which $\mu_L = \mu_R$. In this case, the four self-energies can be written in the form

$$\Sigma_{U:\text{eq}}^{--}(\omega) = [1 - f(\omega)] \Sigma_{U:\text{eq}}^r(\omega) + f(\omega) \Sigma_{U:\text{eq}}^a(\omega), \quad (82)$$

$$\Sigma_{U:\text{eq}}^{++}(\omega) = -f(\omega) \Sigma_{U:\text{eq}}^r(\omega) - [1 - f(\omega)] \Sigma_{U:\text{eq}}^a(\omega), \quad (83)$$

$$\Sigma_{U:\text{eq}}^{-+}(\omega) = f(\omega) \left[\Sigma_{U:\text{eq}}^r(\omega) - \Sigma_{U:\text{eq}}^a(\omega) \right], \quad (84)$$

$$\Sigma_{U:\text{eq}}^{+-}(\omega) = -[1 - f(\omega)] \left[\Sigma_{U:\text{eq}}^r(\omega) - \Sigma_{U:\text{eq}}^a(\omega) \right]. \quad (85)$$

Furthermore, in equilibrium, $F_{dd:\text{eq}}(\omega)$ and $\Omega_{U:\text{eq}}(\omega)$ are determined by the retarded and advanced functions,

$$F_{dd:\text{eq}}(\omega) = [1 - 2f(\omega)] \left[G_{dd:\text{eq}}^r(\omega) - G_{dd:\text{eq}}^a(\omega) \right], \quad (86)$$

$$\Omega_{U:\text{eq}}(\omega) = [1 - 2f(\omega)] \left[\Sigma_{U:\text{eq}}^r(\omega) - \Sigma_{U:\text{eq}}^a(\omega) \right]. \quad (87)$$

Specificity at zero temperature, $\Sigma_{U:\text{eq}}^{-+}(\omega)$ and $\Sigma_{U:\text{eq}}^{+-}(\omega)$ vanish, respectively, at $\omega > \mu$ and $\omega < \mu$, because of the Fermi function in eqs. (84) and (85). Similarly, the Green's functions $G_{dd:\text{eq}}^{-+}(\omega)$ and $G_{dd:\text{eq}}^{+-}(\omega)$ also vanish at $\omega > \mu$ and $\omega < \mu$, respectively. Therefore, at the equilibrium ground state, the usual $T = 0$ formalism which yields a single-component Dyson equation

$$G_{dd:\text{eq}}^{--}(\omega) = G_{dd:\text{eq}}^{(0)--}(\omega) + G_{dd:\text{eq}}^{(0)--}(\omega) \Sigma_{U:\text{eq}}^{--}(\omega) G_{dd:\text{eq}}^{--}(\omega) \quad (88)$$

becomes available.

3.3 Current through the Anderson impurity

The operators for the current flows from the left reservoir to the sample J_L and that from the sample to the right reservoir J_R are given by

$$J_L = ie \sum_{\sigma} v_L \left[d_{\sigma}^{\dagger} c_{L\sigma} - c_{L\sigma}^{\dagger} d_{\sigma} \right], \quad (89)$$

$$J_R = ie \sum_{\sigma} v_R \left[c_{R\sigma}^{\dagger} d_{\sigma} - d_{\sigma}^{\dagger} c_{R\sigma} \right]. \quad (90)$$

As mentioned in Sec. 2.6, the expectation values can be expressed in the form

$$\langle J_L \rangle = 2e \int_{-\infty}^{\infty} \frac{d\omega}{2\pi} v_L \left[G_{Ld}^{-+}(\omega) - G_{dL}^{-+}(\omega) \right], \quad (91)$$

$$\langle J_R \rangle = 2e \int_{-\infty}^{\infty} \frac{d\omega}{2\pi} v_R \left[G_{dR}^{-+}(\omega) - G_{Rd}^{-+}(\omega) \right]. \quad (92)$$

The inter-site Green's functions in the right-hand side of eq. (92) can be expressed in terms of $\mathbf{G}_{dd}(\omega)$ using eqs. (55)–(56), and (61)–(62), as

$$\mathbf{P}^{-1} \mathbf{G}_{Rd} \mathbf{P} = \begin{bmatrix} 0 & G_{Rd}^a \\ G_{Rd}^r & F_{Rd} \end{bmatrix} = -v_R \begin{bmatrix} 0 & g_R^a G_{dd}^a \\ g_R^r G_{dd}^r & g_R^r F_{dd} + F_R^0 G_{dd}^a \end{bmatrix}, \quad (93)$$

$$\mathbf{P}^{-1} \mathbf{G}_{dR} \mathbf{P} = \begin{bmatrix} 0 & G_{dR}^a \\ G_{dR}^r & F_{dR} \end{bmatrix} = -v_R \begin{bmatrix} 0 & G_{dd}^a g_R^a \\ G_{dd}^r g_R^r & G_{dd}^r F_R^0 + F_{dd} g_R^a \end{bmatrix}. \quad (94)$$

Thus, using eqs. (39), (75), and (93)–(94), we obtain

$$\begin{aligned} v_R [G_{dR}^{-+} - G_{Rd}^{-+}] &= \frac{v_R}{2} [F_{dR} - F_{Rd}] \\ &= \frac{v_R^2}{2} \left[(g_R^r - g_R^a) F_{dd} - F_R^0 (G_{dd}^r - G_{dd}^a) \right] \\ &= \Gamma_R G_{dd}^r G_{dd}^a [4\Gamma_L (f_L - f_R) - i\Omega_U - 2(1 - 2f_R) \text{Im}\Sigma_U^r]. \end{aligned} \quad (95)$$

Similarly, for the right-hand side of eq. (91), we obtain

$$\begin{aligned} v_L [G_{Ld}^{-+} - G_{dL}^{-+}] &= \frac{v_L}{2} [F_{Ld} - F_{dL}] \\ &= \frac{v_L^2}{2} \left[-(g_L^r - g_L^a) F_{dd} + F_L^0 (G_{dd}^r - G_{dd}^a) \right] \\ &= \Gamma_L G_{dd}^r G_{dd}^a [4\Gamma_R (f_L - f_R) + i\Omega_U + 2(1 - 2f_L) \text{Im}\Sigma_U^r]. \end{aligned} \quad (96)$$

If the two couplings between the Anderson impurity and leads have a property $\Gamma_L(\omega) = \lambda\Gamma_R(\omega)$ with λ being a constant [15], the expression for current can be simplified by taking an average, $\Gamma_L \times (95) + \Gamma_R \times (96)$, as

$$\begin{aligned} \langle J \rangle &= \frac{\Gamma_L \langle J_R \rangle + \Gamma_R \langle J_L \rangle}{\Gamma_R + \Gamma_L} \\ &= \frac{2e}{h} \int_{-\infty}^{\infty} d\omega [f_L(\omega) - f_R(\omega)] \frac{4\Gamma_L\Gamma_R}{\Gamma_R + \Gamma_L} [-\text{Im} G_{dd}^r(\omega)] . \end{aligned} \quad (97)$$

Note that $\langle J \rangle = \langle J_L \rangle = \langle J_R \rangle$ for stationary states.

3.4 Perturbation expansion with respect to \mathcal{H}_C^U

So far, we have discussed general properties of the nonequilibrium Green's functions. To study how the inter-electron interactions affect the transport properties, the self-energy $\Sigma_U(\omega)$ must be calculated with reliable methods. Because the noninteracting Green's function, which includes the couplings between the leads and the Anderson impurity, have already been obtained in eqs. (68)–(70), the remaining task is calculating $\Sigma_U(\omega)$, for instance, by taking $\mathbf{G}_{dd}^{(0)}$ to be the unperturbed Green's function. Then, the interacting Green's function \mathbf{G}_{dd} are deduced via the Dyson equation (59).

The self-energy $\Sigma_U(\omega)$ can be calculated with the perturbation expansion with respect to the inter-electron interaction \mathcal{H}_C^U . For generating the perturbation series, it is convenient to introduce an effective action,

$$S(\eta^\dagger, \eta) = S_0(\eta^\dagger, \eta) + S_U(\eta^\dagger, \eta) + S_{\text{ex}}(\eta^\dagger, \eta) , \quad (98)$$

$$S_0(\eta^\dagger, \eta) = \sum_{\sigma} \int dt dt' \eta_{\sigma}^{\dagger}(t) \mathbf{K}_{dd}^{(0)}(t, t') \eta_{\sigma}(t') , \quad (99)$$

$$\begin{aligned} S_U(\eta^\dagger, \eta) &= -U \int dt \left[\eta_{\uparrow-}^{\dagger}(t) \eta_{\uparrow-}(t) \eta_{\downarrow-}^{\dagger}(t) \eta_{\downarrow-}(t) \right. \\ &\quad \left. - \eta_{\uparrow+}^{\dagger}(t) \eta_{\uparrow+}(t) \eta_{\downarrow+}^{\dagger}(t) \eta_{\downarrow+}(t) \right] . \end{aligned} \quad (100)$$

Here, $\eta_{\sigma}^{\dagger}(t) = (\eta_{\sigma-}^{\dagger}(t), \eta_{\sigma+}^{\dagger}(t))$ is a two-component Grassmann number corresponding to the $-$ and $+$ branches of the Keldysh contour shown in Fig. 3. The Kernel $\mathbf{K}_{dd}^{(0)}$ is determined by the noninteracting Greens function,

$$\mathbf{K}_{dd}^{(0)}(\omega) \equiv \left\{ \mathbf{G}_{dd}^{(0)}(\omega) \right\}^{-1} , \quad (101)$$

$$\mathbf{K}_{dd}^{(0)}(t, t') = \int \frac{d\omega}{2\pi} \mathbf{K}_{dd}^{(0)}(\omega) e^{-i\omega(t-t')} . \quad (102)$$

In eq. (100), the sign for the interaction along the $-$ branch and that for $+$ branch are different. This correspond to the sign arises in eq. (24), and it is determined from which of the time-evolution operators, $U(+\infty, -\infty)$ or $U(-\infty, +\infty)$, the perturbation terms arise. For $S_{\text{ex}}(\eta^\dagger, \eta)$ in eq. (98), we introduce an external source of two anticommutating c-numbers $\mathbf{j}_\sigma^\dagger(t) = (j_{\sigma-}^\dagger(t), j_{\sigma+}^\dagger(t))$ following along the standard procedure [20],

$$S_{\text{ex}}(\eta^\dagger, \eta) = - \sum_\sigma \int dt \left[\boldsymbol{\eta}_\sigma^\dagger(t) \mathbf{j}_\sigma(t) + \mathbf{j}_\sigma^\dagger(t) \boldsymbol{\eta}_\sigma(t') \right]. \quad (103)$$

In this formulation, the Green's functions are generated from a functional $Z[j]$, as

$$Z[j] \equiv \int D\eta^\dagger D\eta e^{iS(\eta^\dagger, \eta)}, \quad (104)$$

$$G_{dd,\sigma}^{\nu\nu'}(t, t') = -i \frac{1}{Z[0]} \frac{\delta}{\delta j_{\sigma\nu}^\dagger(t)} \frac{\delta}{\delta j_{\sigma\nu'}(t')} Z[j] \Big|_{j=0}. \quad (105)$$

In the noninteracting case, the functional integration can be calculated analytically

$$\begin{aligned} Z^{(0)}[j] &\equiv \int D\eta^\dagger D\eta e^{i[S_0(\eta^\dagger, \eta) + S_{\text{ex}}(\eta^\dagger, \eta)]}, \\ &= Z^{(0)}[0] \exp \left[-i \sum_\sigma \int dt dt' \mathbf{j}_\sigma^\dagger(t) \mathbf{G}_{dd}^{(0)}(t, t') \mathbf{j}_\sigma(t') \right]. \end{aligned} \quad (106)$$

The generating functional $Z[j]$ can be rewritten in the form

$$Z[j] = e^{iS_U\left(-i\frac{\delta}{\delta j}, i\frac{\delta}{\delta j^\dagger}\right)} Z^{(0)}[j]. \quad (107)$$

Here, η and η^\dagger in the action $S_U(\eta^\dagger, \eta)$ has been replaced by the functional derivatives

$$\eta_{\sigma\nu}^\dagger(t) \Rightarrow -i \frac{\delta}{\delta j_{\sigma\nu}(t)}, \quad \eta_{\sigma\nu}(t) \Rightarrow i \frac{\delta}{\delta j_{\sigma\nu}^\dagger(t)}. \quad (108)$$

The perturbation series can be obtained by substituting eq. (106) into (107) and then expanding e^{iS_U} in a power series of S_U .

3.5 Fermi-liquid behavior at low bias voltages

The out-of-equilibrium Anderson model has been studied by a number of theoretical approaches. In this section, we discuss briefly the low-bias behavior of the Green's function and differential conductance, which have been deduced from the Ward identities for the Keldysh formalism [21]. In equilibrium and linear-response regime, the low-energy properties at $\max(\omega, T) \ll T_K$ can be described by the local Fermi liquid theory, where T_K is the Kondo temperature [12]. The results deduced from the Ward identities show that the nonlinear properties at small bias-voltages $eV \ll T_K$ can also be described by the local Fermi liquid theory.

The low-energy behavior of $\text{Im} \Sigma_U^r(\omega)$ has been calculated exactly up to terms of order ω^2 , $(eV)^2$, and T^2 ,

$$\begin{aligned} \text{Im} \Sigma_U^r(\omega) = & -\frac{\pi}{2} \{A_{\text{eq}}(0)\}^3 |\Gamma_{\uparrow\downarrow;\downarrow\uparrow}(0, 0; 0, 0)|^2 \\ & \times \left[(\omega - \alpha eV)^2 + \frac{3\Gamma_L\Gamma_R}{(\Gamma_L + \Gamma_R)^2} (eV)^2 + (\pi T)^2 \right], \end{aligned} \quad (109)$$

where $\Gamma_{\sigma\sigma';\sigma'\sigma}(\omega, \omega'; \omega', \omega)$ is the vertex function for the causal Green's function in the zero-temperature formalism, and $A_{\text{eq}}(\omega) = -\text{Im} G_{dd:\text{eq}}^r(\omega)/\pi$. The parameter α is defined by $\alpha \equiv (\alpha_L\Gamma_L - \alpha_R\Gamma_R)/(\Gamma_L + \Gamma_R)$, where α_L and α_R are constants which have been introduced to specify how the bias voltage is applied to the equilibrium state. Namely, $\mu_L \equiv \alpha_L eV$ and $\mu_R \equiv -\alpha_R eV$ with $\alpha_L + \alpha_R = 1$.

The real part of the self-energy is generally complicated. However, it is simplified in the electron-hole symmetric case for $\epsilon_d = -U/2$, $\Gamma_L = \Gamma_R$, and $\mu_L = -\mu_R = eV/2$. In this case the spectral weight at the Fermi energy becomes $A_{\text{eq}}(0) = 1/(\pi\Delta)$ with $\Delta = \Gamma_L + \Gamma_R$, and the low-energy behavior of the real part of the self-energy is given by

$$\text{Re} \Sigma_U^r(\omega) = (1 - z^{-1})\omega + O(\omega^3), \quad (110)$$

$$z^{-1} \equiv 1 - \left. \frac{\partial \Sigma_{U:\text{eq}}^r(\omega)}{\partial \omega} \right|_{\omega=0}. \quad (111)$$

Here, the constant Hartree term $U/2$ is included into the unperturbed part, and it set the position of the Kondo peak on the Fermi energy $\epsilon_d + U/2 = 0$. Therefore, $G^r(\omega)$ can be deduced exactly up to terms of order ω^2 , T^2 and

$(eV)^2$ from eqs. (109) and (110),

$$G^r(\omega) \simeq \frac{z}{\omega + i\tilde{\Delta} + i\frac{\tilde{U}^2}{2\tilde{\Delta}(\pi\tilde{\Delta})^2} \left[\omega^2 + \frac{3}{4}(eV)^2 + (\pi T)^2 \right]}, \quad (112)$$

where the renormalized parameters are defined by

$$\tilde{\Delta} \equiv z\Delta, \quad \tilde{U} \equiv z^2 \Gamma_{\uparrow\downarrow;\downarrow\uparrow}(0, 0; 0, 0). \quad (113)$$

The order U^2 result [14] can be reproduced from eq. (112) by replacing \tilde{U} with the bare Coulomb interaction U and using the perturbation result for the renormalization factor $z = 1 - (3 - \pi^2/4)u^2 + \dots$, where $u = U/(\pi\Delta)$.

This result shows that in the symmetric case the low-voltage behavior is characterized by the two parameters $\tilde{\Delta}$ and \tilde{U} . These two parameters are defined with respect to the equilibrium ground state, and the exact Bethe ansatz results exist for these parameters. The width of the Kondo resonance $\tilde{\Delta}$ decreases with increasing U , and becomes close to $\tilde{\Delta} \simeq (4/\pi)T_K$ for large U with the Kondo temperature defined by

$$T_K = \pi\Delta\sqrt{u/(2\pi)} \exp[-\pi^2 u/8 + 1/(2u)]. \quad (114)$$

The Wilson ratio is usually defined by $R \equiv \tilde{\chi}_s/\tilde{\gamma}$, where $\tilde{\gamma}$ and $\tilde{\chi}_s$ are the enhancement factors for the T -linear specific heat and spin susceptibility, respectively [11]. Alternatively, it corresponds to the ration of \tilde{U} to $\tilde{\Delta}$,

$$R - 1 = \tilde{U}/(\pi\tilde{\Delta}). \quad (115)$$

The Wilson ratio takes a value $R = 1$ for $U = 0$, and it reaches $R = 2$ in the strong-coupling limit $U \rightarrow \infty$.

The nonequilibrium current $\langle J \rangle$ is calculated by substituting eq. (112) into eq. (97). Then, the differential conductance dJ/dV are determined exactly up to terms of order T^2 and $(eV)^2$,

$$\frac{dJ}{dV} = \frac{2e^2}{h} \left[1 - \frac{1 + 2(R - 1)^2}{3} \left(\frac{\pi T}{\tilde{\Delta}} \right)^2 - \frac{1 + 5(R - 1)^2}{4} \left(\frac{eV}{\tilde{\Delta}} \right)^2 + \dots \right]. \quad (116)$$

Therefore, the nonlinear $(eV)^2$ term is also scaled by the resonance width $\tilde{\Delta}$, and the coefficient is determined by the parameter $R - 1$, or $\tilde{U}/(\pi\tilde{\Delta})$.

4 Transport theory based on Kubo formalism

We have discussed in Sec. 2.6 that in the noninteracting case the nonequilibrium current can be written in a Landauer-type form, as eq. (50). The similar expression has been derived for interacting electrons in a special case, when the couplings between the leads and sample satisfy the condition $\mathbf{\Gamma}^L(\epsilon) = \lambda \mathbf{\Gamma}^R(\epsilon)$ in the notation used in Ref. [15]. For this condition to be held, the interacting sites must be classified into the following two groups: one group consists of the sites that are connected directly to both of the two leads, and other group consists of the sites that have no direct links (hopping matrix elements) to the leads. This condition restricts the application of eq. (50). For instance, if there is an interacting site that is connected to only one of the two leads, the condition is not satisfied. Therefore, eq. (50) is not applicable to a series of quantum dots as illustrated in Fig. 6. Nevertheless, in the linear-response regime, the Landauer-type expression of the dc conductance, eq. (139), can be derived quite generally without the condition mentioned above [19].

In Sec. 4.1, based on the Kubo formalism, we describe the outline of the derivation of eq. (139) for interacting electrons. Our proof uses the analytic properties of the vertex corrections following along the Éliashberg theory of a transport equation for correlated electrons [22, 23]. The many-body transmission probability $\mathcal{T}(\epsilon)$ is given by eq. (140), and it is written in terms of a three-point correlation function. At zero temperature, the imaginary part of the self-energy due to the interaction and the vertex corrections for the current become zero at the Fermi energy $\epsilon = 0$. Due to this property, the transmission probability at $T = 0$ is determined by the single-particle Green's functions as shown in eq. (141). In Sec. 4.2, the current conservation law for the correlation functions is described with the generalized Ward identity, which expresses the relation between the self-energy and current vertex. In Sec. 4.3, we provide the Lehmann representation of the three-point functions to carry out the analytic continuation formally. It can be also used for nonperturbative calculations of $\mathcal{T}(\epsilon)$. We apply this formulation to a finite Hubbard chain in Sec. 4.4, and show an example of the transmission probability $\mathcal{T}(\epsilon)$ for interacting electrons.

4.1 Many-body transmission coefficient $\mathcal{T}(\epsilon)$

We now consider the Hamiltonian $\mathcal{H}_{\text{tot}}^{\text{eq}}$ defined in eq. (1) again, which is also illustrated in Fig. 1. The dc conductance g can be determined in the Kubo formalism, and it corresponds to the ω -linear imaginary part of a current-current correlation function $K_{\alpha\alpha'}(\omega + i0^+)$;

$$g = e^2 \lim_{\omega \rightarrow 0} \frac{K_{\alpha\alpha'}(\omega + i0^+) - K_{\alpha\alpha'}(i0^+)}{i\omega}, \quad (117)$$

$$K_{\alpha\alpha'}(i\nu_l) = \int_0^\beta d\tau \langle T_\tau J_\alpha(\tau) J_{\alpha'}(0) \rangle e^{i\nu_l \tau}, \quad (118)$$

where $\alpha = L$ or R . The retarded correlation can be calculated via the analytic continuation $K_{\alpha\alpha'}(\omega + i0^+) \equiv K_{\alpha\alpha'}(i\nu_l)|_{i\nu_l \rightarrow \omega + i0^+}$, where $\nu_l = 2\pi l/\beta$ is the Matsubara frequency. The current operator J_α is defined by

$$J_L = i \sum_\sigma v_L (c_{1\sigma}^\dagger c_{0\sigma} - c_{0\sigma}^\dagger c_{1\sigma}), \quad (119)$$

$$J_R = i \sum_\sigma v_R (c_{N+1\sigma}^\dagger c_{N\sigma} - c_{N\sigma}^\dagger c_{N+1\sigma}). \quad (120)$$

Here J_L is the current flowing into the sample from the left lead, and J_R is the current flowing out to the right lead from the sample. These currents and total charge in the sample ρ_C satisfy the equation of continuity

$$\rho_C = \sum_{j \in C, \sigma} c_{j\sigma}^\dagger c_{j\sigma}, \quad (121)$$

$$\frac{\partial \rho_C}{\partial t} + J_R - J_L = 0. \quad (122)$$

Owing to this property, the dc conductance g defined in eq. (117) does not depend on the choice of α and α' [18]. Note that $K_{\alpha'\alpha}(z) = K_{\alpha\alpha'}(z)$ owing to the time-reversal symmetry of \mathcal{H} .

To calculate the ω -linear imaginary part of $K_{\alpha\alpha'}(\omega + i0^+)$, we introduce the three-point correlation functions of the charge and currents,

$$\Phi_{C;jj'}(\tau; \tau_1, \tau_2) = \langle T_\tau \delta\rho_C(\tau) c_{j\sigma}(\tau_1) c_{j'\sigma}^\dagger(\tau_2) \rangle, \quad (123)$$

$$\Phi_{L;jj'}(\tau; \tau_1, \tau_2) = \langle T_\tau J_L(\tau) c_{j\sigma}(\tau_1) c_{j'\sigma}^\dagger(\tau_2) \rangle, \quad (124)$$

$$\Phi_{R;jj'}(\tau; \tau_1, \tau_2) = \langle T_\tau J_R(\tau) c_{j\sigma}(\tau_1) c_{j'\sigma}^\dagger(\tau_2) \rangle, \quad (125)$$

where $\delta\rho_C \equiv \rho_C - \langle \rho_C \rangle$. These three functions can be expressed as functions of two Matsubara frequencies $i\nu$ and $i\varepsilon$,

$$\Phi_{\gamma;jj'}(\tau; \tau_1, \tau_2) = \frac{1}{\beta^2} \sum_{i\varepsilon, i\nu} \Phi_{\gamma;jj'}(i\varepsilon, i\varepsilon + i\nu) e^{-i\varepsilon(\tau_1 - \tau)} e^{-i(\varepsilon + \nu)(\tau - \tau_2)}, \quad (126)$$

for $\gamma = C, L, R$. We mainly consider the electrons in the central region assuming $jj' \in C$. In the right-hand side of eqs. (124) and (125), there still exist the creation and annihilation operators with respect to the leads at 0 and $N+1$ in the operators J_L and J_R . The correlation functions that include these two sites as one of the external points can be related to those defined with respect to the adjacent sites 1 and N , by using the properties of the Green's function at the two interfaces:

$$\begin{cases} G_{0,j}(z) &= -g_L(z) v_L G_{1,j}(z) & \text{for } 1 \leq j \leq N+1 \\ G_{j,N+1}(z) &= -G_{j,N}(z) v_R g_R(z) & \text{for } 0 \leq j \leq N \end{cases}. \quad (127)$$

Here $g_L(z)$ and $g_R(z)$ are the local Green's functions at the interfaces of the isolated leads, 0 and $N+1$, respectively. Using these properties, the three-point correlation functions for $jj' \in C$ can be expressed as

$$\Phi_{\gamma;jj'}(i\varepsilon, i\varepsilon + i\nu) = \sum_{j_4 j_1 \in C} G_{jj_4}(i\varepsilon) \Lambda_{\gamma;j_4 j_1}(i\varepsilon, i\varepsilon + i\nu) G_{j_1 j'}(i\varepsilon + i\nu), \quad (128)$$

where $\Lambda_{\gamma;j_4 j_1}$ includes all the vertex corrections. The corresponding bare current vertices are given by

$$\Lambda_{C;j_4 j_1}^{(0)}(i\varepsilon, i\varepsilon + i\nu) = \delta_{j_4, j_1}, \quad (129)$$

$$\Lambda_{L;j_4 j_1}^{(0)}(i\varepsilon, i\varepsilon + i\nu) = \lambda_L(i\varepsilon, i\varepsilon + i\nu) \delta_{1, j_4} \delta_{1, j_1}, \quad (130)$$

$$\Lambda_{R;j_4 j_1}^{(0)}(i\varepsilon, i\varepsilon + i\nu) = \lambda_R(i\varepsilon, i\varepsilon + i\nu) \delta_{N, j_4} \delta_{N, j_1}, \quad (131)$$

with

$$\lambda_L(i\varepsilon, i\varepsilon + i\nu) = -i v_L^2 [g_L(i\varepsilon + i\nu) - g_L(i\varepsilon)], \quad (132)$$

$$\lambda_R(i\varepsilon, i\varepsilon + i\nu) = i v_R^2 [g_R(i\varepsilon + i\nu) - g_R(i\varepsilon)], \quad (133)$$

We now calculate the ω -linear part of $K_{\alpha\alpha'}(z)$ taking α and α' to be R and L , respectively. Using the three-point correlation functions, the current-current correlation function $K_{RL}(i\nu)$ can be expressed as

$$K_{RL}(i\nu) = \frac{1}{\beta} \sum_{i\varepsilon} \sum_{\sigma} \lambda_L(i\varepsilon, i\varepsilon + i\nu) \Phi_{R;11}(i\varepsilon, i\varepsilon + i\nu). \quad (134)$$

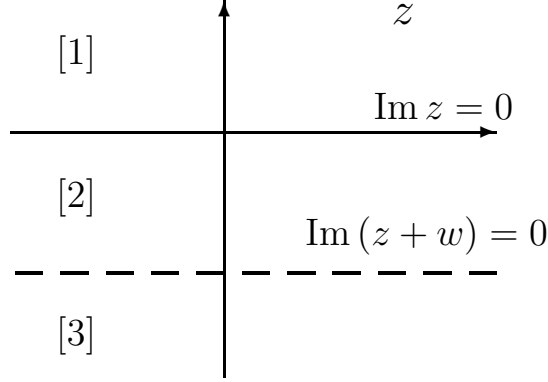


Figure 5: Three analytic regions of $\Phi_{R;11}(z, z+w)$.

Paying attention to the analytic properties of the Green's functions, the summation over the Matsubara frequency can be rewritten in a contour-integral form. Then, by carrying out the analytic continuation $i\nu \rightarrow \omega + i0^+$, we obtain

$$\begin{aligned}
& K_{RL}(\omega + i0^+) \\
&= \sum_{\sigma} \left\{ - \int_{-\infty}^{\infty} \frac{d\epsilon}{2\pi i} f(\epsilon) \lambda_L^{[1]}(\epsilon, \epsilon + \omega) \Phi_{R;11}^{[1]}(\epsilon, \epsilon + \omega) \right. \\
&\quad - \int_{-\infty}^{\infty} \frac{d\epsilon}{2\pi i} [f(\epsilon + \omega) - f(\epsilon)] \lambda_L^{[2]}(\epsilon, \epsilon + \omega) \Phi_{R;11}^{[2]}(\epsilon, \epsilon + \omega) \\
&\quad \left. + \int_{-\infty}^{\infty} \frac{d\epsilon}{2\pi i} f(\epsilon + \omega) \lambda_L^{[3]}(\epsilon, \epsilon + \omega) \Phi_{R;11}^{[3]}(\epsilon, \epsilon + \omega) \right\}, \quad (135)
\end{aligned}$$

where $f(\epsilon) = (e^{\beta\epsilon} + 1)^{-1}$. The superscript with the bracket, that is, $[k]$ for $k = 1, 2, 3$, is introduced specifies the three analytic region of $\Phi_{R;11}(z, z+w)$ and $\lambda_L(z, z+w)$ in the complex z -plane. These regions are separated by the two lines, $\text{Im}(z) = 0$ and $\text{Im}(z+w) = 0$, as shown in Fig 5. In each of the three regions, $\Phi_{R;11}(z, z+w)$ corresponds to the analytic function given by

$$\begin{cases}
\Phi_{R;11}^{[1]}(\epsilon, \epsilon + \omega) = \Phi_{R;11}(\epsilon + i0^+, \epsilon + \omega + i0^+) \\
\Phi_{R;11}^{[2]}(\epsilon, \epsilon + \omega) = \Phi_{R;11}(\epsilon - i0^+, \epsilon + \omega + i0^+) \\
\Phi_{R;11}^{[3]}(\epsilon, \epsilon + \omega) = \Phi_{R;11}(\epsilon - i0^+, \epsilon + \omega - i0^+)
\end{cases} \quad (136)$$

These analytic properties can be clarified explicitly in the Lehmann representation, eq. (158), provided in the next subsection. Similarly, the analytic

continuation of the bare current vertex $\lambda_\alpha(i\varepsilon, i\varepsilon + i\nu)$ for $\alpha = L, R$ is given by

$$\begin{cases} \lambda_\alpha^{[1]}(\epsilon, \epsilon + \omega) = i s_\alpha v_\alpha^2 [g_\alpha^+(\epsilon + \omega) - g_\alpha^+(\epsilon)] \\ \lambda_\alpha^{[2]}(\epsilon, \epsilon + \omega) = i s_\alpha v_\alpha^2 [g_\alpha^+(\epsilon + \omega) - g_\alpha^-(\epsilon)] \\ \lambda_\alpha^{[3]}(\epsilon, \epsilon + \omega) = i s_\alpha v_\alpha^2 [g_\alpha^-(\epsilon + \omega) - g_\alpha^-(\epsilon)] \end{cases}, \quad (137)$$

where the factor s_α is defined such that $s_L = -1$ and $s_R = +1$. In this section, we distinguish the retarded and advanced Green's functions by the label $+$ and $-$, respectively, in the superscript. In the limit of $\omega \rightarrow 0$, the bare vertices for $k = 1$ and 3 vanish as $\lambda_\alpha^{[k]}(\epsilon, \epsilon + \omega) \propto \omega$. In contrast, for $k = 2$, it tends to a finite constant $\lambda_\alpha^{[2]}(\epsilon, \epsilon) = 2 s_\alpha \Gamma_\alpha(\epsilon)$ with $\Gamma_\alpha(\epsilon) = -v_\alpha^2 \text{Im}[g_\alpha^+(\epsilon)]$. Correspondingly, the asymptotic behavior of $\Phi_\alpha^{[k]}(\epsilon, \epsilon + \omega)$ for small ω has been investigated by using the Lehmann representation of a four-point vertex function [22, 23], and the result is [19],

$$\Phi_\alpha^{[k]}(\epsilon, \epsilon + \omega) \propto \begin{cases} \omega & \text{for } k = 1 \\ \text{finite} & \text{for } k = 2 \\ \omega & \text{for } k = 3 \end{cases}, \quad (138)$$

for $\alpha = L, R$. Therefore, taking the $\omega \rightarrow 0$ limit in eq. (117) by using eq. (135) for $K_{RL}(\omega + i0^+)$, we obtain

$$g = \frac{2e^2}{h} \int d\epsilon \left(-\frac{\partial f}{\partial \epsilon} \right) \mathcal{T}(\epsilon), \quad (139)$$

$$\mathcal{T}(\epsilon) = 2 \Gamma_L(\epsilon) \Phi_{R;11}^{[2]}(\epsilon, \epsilon). \quad (140)$$

Thus, the dc conductance is determined by the three-point function for the analytic region $k = 2$. The analytic continuation is performed formally by using the Lehmann representation in Sec. 4.3. The result shows that $\Phi_{R;11}^{[2]}(\epsilon, \epsilon)$ can be expressed as a Fourier transform, eq. (162), of a real-time retarded product in eq. (160).

Specifically, at $T = 0$ the conductance is determined by the value of the transmission probability at the Fermi $\epsilon = 0$, and it can be written in the form [24, 25, 26, 27],

$$\mathcal{T}(0) = 4 \Gamma_L(0) G_{LN}^-(0) \Gamma_R(0) G_{N1}^+(0). \quad (141)$$

This is due to the property that the vertex corrections for the current vanishes at $T = 0$ and $\epsilon = 0$, as shown in eq. (154) in Sec. 4.2. Furthermore, the

reflection probability is given by

$$\mathcal{R}(0) = \left| 1 - 2i\Gamma_L(0)G_{11}^+(0) \right|^2 = \left| 1 - 2i\Gamma_R(0)G_{NN}^+(0) \right|^2. \quad (142)$$

The current conservation $\mathcal{T}(0) + \mathcal{R}(0) = 1$ follows from the identity in eq. (156). Similarly, at zero temperature, the Friedel sum rule for interacting electrons is given by [28],

$$\Delta N_{\text{tot}} = \frac{1}{\pi i} \log[\det \mathbf{S}], \quad (143)$$

where the S -matrix is defined by

$$\mathbf{S} = \begin{bmatrix} 1 - 2i\Gamma_L(0)G_{11}^+(0) & -2i\Gamma_L(0)G_{1N}^+(0) \\ -2i\Gamma_R(0)G_{N1}^+(0) & 1 - 2i\Gamma_R(0)G_{NN}^+(0) \end{bmatrix}. \quad (144)$$

In eq. (143), ΔN_{tot} is the displacement of the total charge defined by

$$\begin{aligned} \Delta N_{\text{tot}} &= \sum_{i \in C} \sum_{\sigma} \langle c_{i\sigma}^{\dagger} c_{i\sigma} \rangle \\ &+ \sum_{i \in L} \sum_{\sigma} \left[\langle c_{i\sigma}^{\dagger} c_{i\sigma} \rangle - \langle c_{i\sigma}^{\dagger} c_{i\sigma} \rangle_L \right] + \sum_{i \in R} \sum_{\sigma} \left[\langle c_{i\sigma}^{\dagger} c_{i\sigma} \rangle - \langle c_{i\sigma}^{\dagger} c_{i\sigma} \rangle_R \right], \end{aligned} \quad (145)$$

where $\langle \dots \rangle_L$ and $\langle \dots \rangle_R$ denote the ground-state average of isolated leads determined by \mathcal{H}_L and \mathcal{H}_R , respectively.

4.2 Current Conservation and Ward identity

The inter-electron interactions generally cause the damping of excitations. Therefore, theoretically, the self-energy and vertex corrections must be treated consistently with the approaches that conserve the current. In this subsection, we discuss the current conservation using a generalized Ward identity.

The generalized Ward identity can be derived from the equation of continuity in the Matsubara form $-(\partial/\partial\tau)\delta\rho_C + iJ_R - iJ_L = 0$ [29],

$$\begin{aligned} -\frac{\partial}{\partial\tau} \Phi_{C;jj'}(\tau; \tau_1, \tau_2) + i\Phi_{R;jj'}(\tau; \tau_1, \tau_2) - i\Phi_{L;jj'}(\tau; \tau_1, \tau_2) \\ = \delta(\tau - \tau_2) G_{jj'}(\tau_1, \tau) - \delta(\tau_1 - \tau) G_{jj'}(\tau, \tau_2). \end{aligned} \quad (146)$$

It can be expressed by using a $N \times N$ matrix representation for $jj' \in C$ with the Matsubara frequencies,

$$\begin{aligned} i\nu \Phi_C(i\varepsilon, i\varepsilon + i\nu) + i\Phi_R(i\varepsilon, i\varepsilon + i\nu) - i\Phi_L(i\varepsilon, i\varepsilon + i\nu) \\ = \mathbf{G}(i\varepsilon) - \mathbf{G}(i\varepsilon + i\nu). \end{aligned} \quad (147)$$

Here, $\mathbf{G}(z) = \{G_{jj'}(z)\}$ and $\Phi_\gamma(z, z+w) = \{\Phi_{\gamma;jj'}(z, z+w)\}$. The matrix version of eq. (128) is given by

$$\Phi_\gamma(z, z+w) = \mathbf{G}(z) \mathbf{\Lambda}_\gamma(z, z+w) \mathbf{G}(z+w). \quad (148)$$

Thus, the identity can also be expressed using $\mathbf{\Lambda}_\gamma(z, z+w) = \{\Lambda_{\gamma;jj'}(z, z+w)\}$, as

$$\begin{aligned} i\nu \mathbf{\Lambda}_C(i\varepsilon, i\varepsilon + i\nu) + i \mathbf{\Lambda}_R(i\varepsilon, i\varepsilon + i\nu) - i \mathbf{\Lambda}_L(i\varepsilon, i\varepsilon + i\nu) \\ = \{\mathbf{G}(i\varepsilon + i\nu)\}^{-1} - \{\mathbf{G}(i\varepsilon)\}^{-1}. \end{aligned} \quad (149)$$

Furthermore, the Dyson equation for the single-particle Green's function can be expressed as

$$\{\mathbf{G}(z)\}^{-1} = z \mathbf{1} - \mathcal{H}_C^0 - \mathbf{V}_{\text{mix}}(z) - \mathbf{\Sigma}(z), \quad (150)$$

$$\mathcal{H}_C^0 = \begin{bmatrix} -t_{11}^C - \mu & -t_{12}^C & \cdots & & \\ -t_{21}^C & -t_{22}^C - \mu & & & \\ \vdots & & \ddots & & \\ & & & & -t_{NN}^C - \mu \end{bmatrix}, \quad (151)$$

$$\mathbf{V}_{\text{mix}}(z) = \begin{bmatrix} v_L^2 g_L(z) & 0 & \cdots & 0 & 0 \\ 0 & 0 & \cdots & 0 & 0 \\ \vdots & \vdots & \ddots & \vdots & \vdots \\ 0 & 0 & \cdots & 0 & 0 \\ 0 & 0 & \cdots & 0 & v_R^2 g_R(z) \end{bmatrix}, \quad (152)$$

and $\mathbf{\Sigma}(z) = \{\Sigma_{jj'}(z)\}$ is the self-energy due to the inter-electron interactions. Therefore, eq. (149) represents a relation between the self-energy and vertex functions, and this identity must be satisfied in the conserving approaches. Carrying out the analytic continuation of eq. (149) in the region $k = 2$, $i\varepsilon + i\nu \rightarrow \epsilon + \omega + i0^+$ and $i\varepsilon \rightarrow \epsilon - i0^+$, and then taking the limit of $\omega \rightarrow 0$, we obtain

$$\mathbf{\Lambda}_R^{[2]}(\epsilon, \epsilon) - \mathbf{\Lambda}_L^{[2]}(\epsilon, \epsilon) = -2 \text{Im} \mathbf{V}_{\text{mix}}^+(\epsilon) - 2 \text{Im} \mathbf{\Sigma}^+(\epsilon) \quad (153)$$

At $T = 0$, $\epsilon = 0$, the imaginary part of the self-energy vanishes $\text{Im} \mathbf{\Sigma}^+(0) = 0$, and then the current vertices become equal to the bare ones,

$$\Lambda_{R;j_4 j_1}^{[2]}(0, 0) = 2 \Gamma_R(0) \delta_{N j_4} \delta_{N j_1}, \quad (154)$$

$$\Lambda_{L;j_4 j_1}^{[2]}(0, 0) = -2 \Gamma_L(0) \delta_{1 j_4} \delta_{1 j_1}. \quad (155)$$

Correspondingly, $\Phi_{R;11}^{[2]}(0,0) = G_{1N}^-(0)2\Gamma_R(0)G_{N1}^+(0)$ at $T = 0$, and then the transmission probability is given by eq. (141). Alternatively, at $T = 0$, the analytic continuation of eq. (146) in region $k = 2$ is written in the form

$$\mathbf{G}^+(0) - \mathbf{G}^-(0) = \mathbf{G}^+(0) \left[\mathbf{V}_{\text{mix}}^+(0) - \mathbf{V}_{\text{mix}}^-(0) \right] \mathbf{G}^-(0), \quad (156)$$

and the $(1,1)$ and (N,N) matrix elements represent the optical theorem for eqs. (141) and (142).

Particularly, for the single Anderson impurity at $N = 1$, eq. (147) becomes a single-component equation with respect to the impurity site. In the region $k = 2$, it becomes $\Phi_R^{[2]}(\epsilon, \epsilon) - \Phi_L^{[2]}(\epsilon, \epsilon) = G^-(\epsilon) - G^+(\epsilon)$ in the limit of $\omega \rightarrow 0$. Furthermore, if the mixing terms have a property $\Gamma_L(\epsilon) = \lambda \Gamma_R(\epsilon)$, an additional relation $\Phi_L^{[2]}(\epsilon, \epsilon) = -\lambda \Phi_R^{[2]}(\epsilon, \epsilon)$ follows. Thus, in this case the dc conductance can be written in the form [14, 15],

$$g_{\text{single}} = \frac{2e^2}{h} \int_{-\infty}^{\infty} d\epsilon \left(-\frac{\partial f}{\partial \epsilon} \right) \frac{4\Gamma_L\Gamma_R}{\Gamma_R + \Gamma_L} \left[-\text{Im} G^+(\epsilon) \right]. \quad (157)$$

4.3 Lehmann representation for $\mathcal{T}(\epsilon)$

We now show that the transmission probability $\mathcal{T}(\epsilon)$ can be expressed in terms of a real-time retarded product in eq. (160) via the Fourier transform eq. (162). It shows a direct link between the transmission probability and dynamic correlation functions. To prove it, we first of all derive the Lehmann representation for $\Phi_{R;11}(i\varepsilon, i\varepsilon + i\nu)$, and then carry out the analytical continuation.

Inserting a complete set of the eigenstates, $\mathcal{H}|n\rangle = E_n|n\rangle$, into eq. (125) and using eq. (126), we obtain

$$\begin{aligned} \Phi_{R;11}(i\varepsilon, i\varepsilon + i\nu) &= \frac{1}{Z} \sum_{lmn} \langle l|c_{1\sigma}^\dagger|m\rangle \langle m|J_R|n\rangle \langle n|c_{1\sigma}|l\rangle \\ &\quad \times \left[\frac{e^{-\beta E_m}}{(i\varepsilon + i\nu + E_m - E_l)(i\nu + E_m - E_n)} \right. \\ &\quad \left. - \frac{e^{-\beta E_l}}{(i\varepsilon + E_n - E_l)(i\varepsilon + i\nu + E_m - E_l)} \right. \\ &\quad \left. - \frac{e^{-\beta E_n}}{(i\nu + E_m - E_n)(i\varepsilon + E_n - E_l)} \right] \end{aligned}$$

$$\begin{aligned}
& + \frac{1}{Z} \sum_{lmn} \langle l | c_{1\sigma} | n \rangle \langle n | J_R | m \rangle \langle m | c_{1\sigma}^\dagger | l \rangle \\
& \times \left[\frac{e^{-\beta E_n}}{(i\varepsilon + E_l - E_n)(i\nu + E_n - E_m)} \right. \\
& \quad + \frac{e^{-\beta E_l}}{(i\varepsilon + E_l - E_n)(i\varepsilon + i\nu + E_l - E_m)} \\
& \quad \left. - \frac{e^{-\beta E_m}}{(i\varepsilon + i\nu + E_l - E_m)(i\nu + E_n - E_m)} \right], \quad (158)
\end{aligned}$$

where $Z = \text{Tr} e^{-\beta \mathcal{H}}$. From eq. (158), the analytic continuation to obtain $\Phi_{R;11}^{[k]}(\epsilon, \epsilon + \omega)$ for $k = 1, 2, 3$ can be carried out by replacing the imaginary frequencies $i\varepsilon$ and $i\nu$ by the real ones ϵ and ω , respectively, with the infinitesimal imaginary parts shown in eq. (136). Then the same expressions for $\Phi_{R;11}^{[k]}(\epsilon, \epsilon + \omega)$ can be derived from the real-time functions

$$\begin{aligned}
\Phi_{R;11}^{[1]}(t; t_1, t_2) &= \theta(t - t_1) \theta(t_1 - t_2) \left\langle \left[\left\{ c_{1\sigma}(t_1), c_{1\sigma}^\dagger(t_2) \right\}, J_R(t) \right] \right\rangle \\
& \quad + \theta(t_1 - t) \theta(t - t_2) \left\langle \left\{ c_{1\sigma}(t_1), \left[c_{1\sigma}^\dagger(t_2), J_R(t) \right] \right\} \right\rangle, \quad (159)
\end{aligned}$$

$$\begin{aligned}
\Phi_{R;11}^{[2]}(t; t_1, t_2) &= \theta(t - t_1) \theta(t_1 - t_2) \left\langle \left\{ c_{1\sigma}^\dagger(t_2), \left[c_{1\sigma}(t_1), J_R(t) \right] \right\} \right\rangle \\
& \quad - \theta(t - t_2) \theta(t_2 - t_1) \left\langle \left\{ c_{1\sigma}(t_1), \left[c_{1\sigma}^\dagger(t_2), J_R(t) \right] \right\} \right\rangle, \quad (160)
\end{aligned}$$

$$\begin{aligned}
\Phi_{R;11}^{[3]}(t; t_1, t_2) &= -\theta(t - t_2) \theta(t_2 - t_1) \left\langle \left[\left\{ c_{1\sigma}(t_1), c_{1\sigma}^\dagger(t_2) \right\}, J_R(t) \right] \right\rangle \\
& \quad - \theta(t_2 - t) \theta(t - t_1) \left\langle \left\{ c_{1\sigma}^\dagger(t_2), \left[c_{1\sigma}(t_1), J_R(t) \right] \right\} \right\rangle, \quad (161)
\end{aligned}$$

where $J_R(t) \equiv e^{i\mathcal{H}t} J_R e^{-i\mathcal{H}t}$, and $\theta(t)$ is the step function. The commutators are defined by $[A, B] \equiv AB - BA$, and $\{A, B\} \equiv AB + BA$, as usual. The Fourier transform into the real frequencies is given by

$$\begin{aligned}
& \int_{-\infty}^{\infty} dt dt_1 dt_2 e^{i\omega t} e^{i\epsilon t_1} e^{-i\epsilon' t_2} \Phi_{R;11}^{[k]}(t; t_1, t_2) \\
& = 2\pi \delta(\epsilon + \omega - \epsilon') \Phi_{R;11}^{[k]}(\epsilon, \epsilon + \omega). \quad (162)
\end{aligned}$$

For example, a time-ordered function

$$F(t; t_1, t_2) = \theta(t - t_1) \theta(t_1 - t_2) \left\langle J_R(t) c_{1\sigma}(t_1) c_{1\sigma}^\dagger(t_2) \right\rangle \quad (163)$$

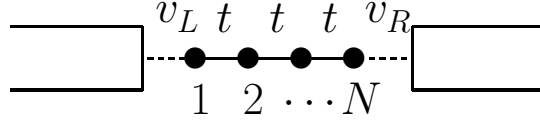


Figure 6: Schematic picture of a finite Hubbard chain.

is transformed into

$$F(\epsilon, \epsilon + \omega) = \frac{-1}{Z} \sum_{lmn} \frac{e^{-\beta E_m} \langle l | c_{1\sigma}^\dagger | m \rangle \langle m | J_R | n \rangle \langle n | c_{1\sigma} | l \rangle}{(\epsilon + \omega + E_m - E_l + i0^+)(\omega + E_m - E_n + i0^+)}. \quad (164)$$

Among the three real-time functions eqs. (159)–(161), the function for the region $k = 2$, that is, $\Phi_{R;11}^{[2]}(t; t_1, t_2)$ in eq. (160) determines the transmission probability $\mathcal{T}(\epsilon) = 2\Gamma_L(\epsilon) \Phi_{R;11}^{[2]}(\epsilon, \epsilon)$. Because the analytic continuation has already been done, the real-time correlation links directly to the transport coefficient. This formulation can be used for numerical calculations.

4.4 Application to a Hubbard chain connected to leads

In this subsection, we apply the linear-response formulation to a finite Hubbard chain attached to reservoirs, which can be considered as a model for a series of quantum dots or atomic wires of nanometer size. A schematic picture of the model is shown in Fig. 6. The Hamiltonian parameters defined in eq. (1) are taken as follows. We take t_{ij}^C to be the nearest-neighbor hopping t , and $U_{j_1 j_2; j_2 j_1}$ to be an onsite repulsion U . Specifically, we consider the electron-hole symmetric case, at which $\mu = 0$ and $\epsilon_d + U/2 = 0$ with ϵ_d being the onsite energy. We also assume that the two couplings are symmetric $\Gamma_L = \Gamma_R (\equiv \Gamma)$, a

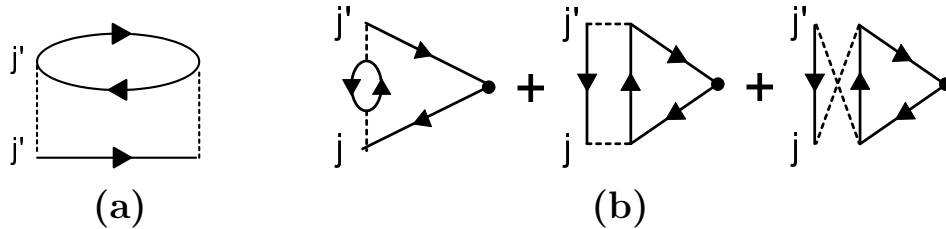


Figure 7: The order U^2 terms of (a) self-energy and (b) vertex corrections.

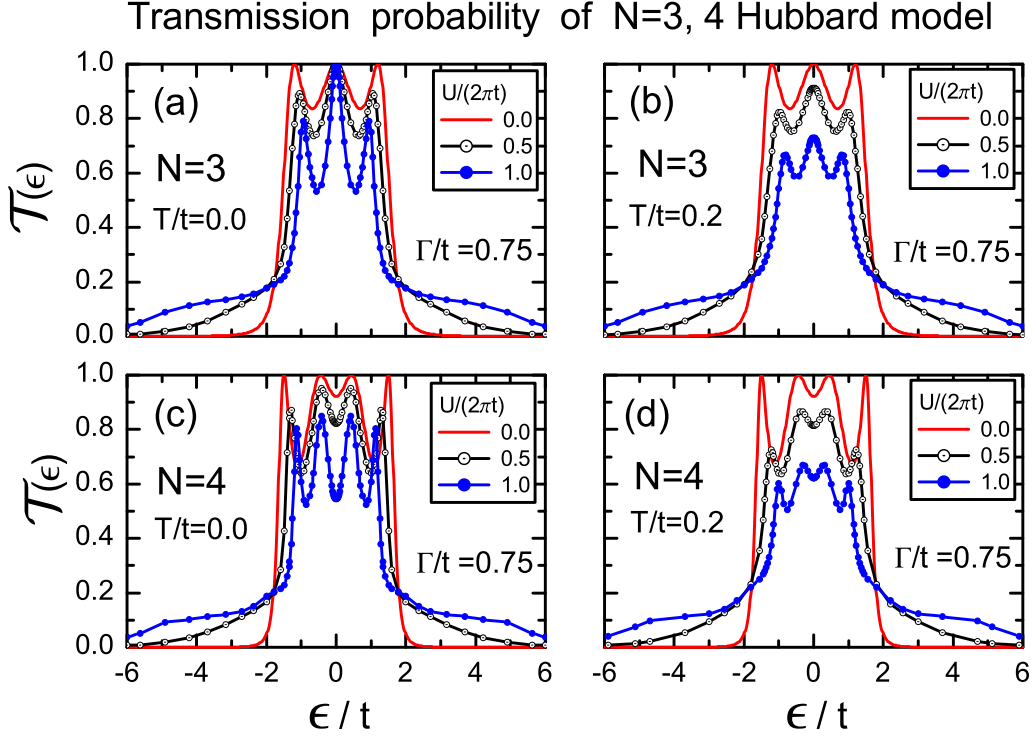


Figure 8: Many-body transmission coefficient for $N = 3$ (upper two panels) and 4 (lower two panels) is plotted vs ϵ/t for $\Gamma/t = 0.75$ for three values of $U/(2\pi t)$; (—) 0.0, (—○—) 0.5, and (—●—) 1.0. The temperature is taken to be $T/t = 0.0$ for (a) and (c), and $T/t = 0.2$ for (b) and (d).

To examine the effects of the Coulomb interaction, we calculate the self-energy and vertex corrections up to terms of order U^2 , the Feynman diagrams for which are illustrated in Fig. 7 [19]. These contributions satisfy the generalized Ward identity eq. (153) that corresponds to the current conservation law. In Fig. 8, the results of $\mathcal{T}(\epsilon)$ for $N = 3, 4$ are plotted vs ϵ/t for $\Gamma/t = 0.75$ for three values of $U/(2\pi t)$; (—) 0.0, (—○—) 0.5, and (—●—) 1.0. The temperature T/t is taken to be (a) 0.0, (b) 0.2 for $N = 3$ in the upper panels, and (c) 0.0, (d) 0.2 for $N = 4$ in the lower panels.

At low temperatures, there are N resonance peaks that have one-to-one correspondence to resonant states of the unperturbed system. In addition

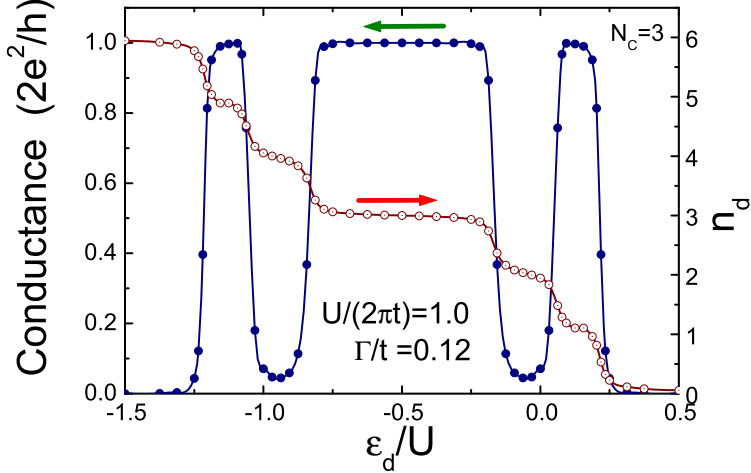


Figure 9: NRG results of the conductance g and the number of electrons n_d in triple dots $N = 3$ as functions of ϵ_d at $T = 0.0$.

to these resonance peaks, two broad peaks of atomic character appear at $\epsilon \simeq \pm U/2$ for large U . The resonance peaks become sharper with increasing U at low temperatures as seen in the panels (a) and (c). However, the height of the peaks decreases with increasing U . One exception, which happens for odd N , is the Kondo resonance at the Fermi level $\epsilon = 0$. At this peak the transmission probability reaches the unitary-limit value 1.0 for any values of U , when the systems have the inversion symmetry $\Gamma_L = \Gamma_R$ together with the electron-hole symmetry [27, 30]. The width of the Kondo resonance T_K must decrease with increasing N . For even N , the transmission probability $\mathcal{T}(\epsilon)$ shows a minimum at $\epsilon = 0$. The characteristic energy scale in this case is the width of the valley, which eventually becomes the Mott-Hubbard gap in the limit of large N . The high energy profile of $\mathcal{T}(\epsilon)$ at $|\epsilon| \gtrsim 2t$ in the case of $N = 3$ is similar to that for $N = 4$. Namely, the high-energy part shows no notable N dependence. For $U/(2\pi t) = 0.5$, the upper and lower Hubbard levels at $\epsilon \simeq \pm U/2$ exist inside the energy region corresponding to the one-dimensional band of the width $2t$. The two Hubbard levels got outside of this energy region for $U/2 \gtrsim 2t$. At finite temperatures, the resonance peaks at

$|\epsilon| \lesssim 2t$ become broad, and the peak height decreases with increasing T . The structures of the resonance peaks vanish eventually at higher temperatures, and then the even-odd oscillatory behavior disappears [19].

Recently, there has been a numerical progress in this subject. The conductance for $N = 3$ and that of 4 have been calculated away from half-filling as functions of ϵ_d with numerical renormalization group (NRG). It has been clarified that the conductance shows a typical Kondo behavior as seen in Fig. 9. Namely, the plateau of the Unitary limit $g \simeq 2e^2/h$ emerges at the gate voltages, ϵ_d , corresponding to odd-number occupations of the electrons. In contrast, the conductance shows wide minimum when the interacting region is occupied by electrons of even numbers [31, 32].

5 Tomonaga-Luttinger Model

Transport through interacting systems in one dimension has been studied extensively for quantum wires, organic conductors, carbon nanotube, etc. In this section, we provide a brief introduction to a Tomonaga-Luttinger model [33], to take a quick look at the transport properties of a typical interacting system in one dimension.

5.1 Spin-less fermions in one dimension

We start with the spin-less fermions described by the Hamiltonian,

$$H_0 - \langle H_0 \rangle_0 = \sum_k (\epsilon_k - \mu) \left[c_k^\dagger c_k - \langle c_k^\dagger c_k \rangle_0 \right], \quad (165)$$

$$H_I = \frac{1}{2L} \sum_{qkk'} V_q c_{k+q}^\dagger c_{k'-q}^\dagger c_{k'} c_k. \quad (166)$$

In eq. (165), the ground-state energy for the noninteracting electrons has been subtracted. At low energies, the excitations near the Fermi level play a dominant role, so that ϵ_k can be linearized at the two Fermi points $k = \pm k_F$,

$$\begin{aligned} \mathcal{H}_0 = & \sum_k v_F(k - k_F) \left[a_k^\dagger a_k - \langle a_k^\dagger a_k \rangle_0 \right] \\ & + \sum_k v_F(-k - k_F) \left[b_k^\dagger b_k - \langle b_k^\dagger b_k \rangle_0 \right]. \end{aligned} \quad (167)$$

Here a_k (b_k) is the operator for the right-moving (left-moving) particles. The summation over k in eq. (167) should be restricted in a range $|k| -$

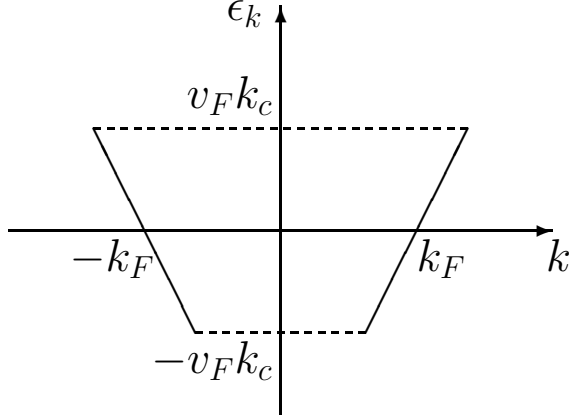


Figure 10: Linearized dispersion

$k_F < k_c$ with the cut-off momentum k_c of the order a band width $D \sim v_F k_c$ as illustrated in Fig. 5.1. However, we assume that $k_c \rightarrow \infty$, and will introduce the cut-off for the momentum transfer q , when it is required [33]. For low-energy properties, the interactions between the electrons near the Fermi level is important. Therefore, the interaction Hamiltonian eq. (166) can be simplified by taking only the scattering processes in which all the four momentums are close to one of the two Fermi points, that is, $k + q \simeq \pm k_F$, $k' - q \simeq \pm k_F$, $k' \simeq \pm k_F$, and $k \simeq \pm k_F$, into account;

$$H_I \simeq \frac{1}{2L} \left(\sum_{q \simeq 0} V_q + \sum_{q \simeq \pm 2k_F} V_q \right) \left(\sum_{k \simeq k_F} + \sum_{k \simeq -k_F} \right) \left(\sum_{k' \simeq k_F} + \sum_{k' \simeq -k_F} \right) c_{k+q}^\dagger c_{k'-q}^\dagger c_{k'} c_k. \quad (168)$$

For the scattering process with small momentum transfer $q \simeq 0$, there are two types of possibilities for the initial momentums $k \simeq k'$ and $k \simeq -k'$. In contrast, in the case of the back scattering $q \simeq \pm 2k_F$, the incident momentums must have the opposite sign $k \simeq -k'$. These scattering processes can be described by a simplified Hamiltonian,

$$H_I \Rightarrow \mathcal{H}_4 + \mathcal{H}_2 + \mathcal{H}_1, \quad (169)$$

$$\mathcal{H}_4 = \frac{g_4}{2L} \sum_{qkk'} a_{k+q}^\dagger a_{k'-q}^\dagger a_{k'} a_k + \frac{g_4}{2L} \sum_{qkk'} b_{k+q}^\dagger b_{k'-q}^\dagger b_{k'} b_k, \quad (170)$$

$$\mathcal{H}_2 = \frac{g_2}{2L} \sum_{qkk'} a_{k+q}^\dagger b_{k'-q}^\dagger b_{k'} a_k + \frac{g_2}{2L} \sum_{qkk'} b_{k+q}^\dagger a_{k'-q}^\dagger a_{k'} b_k, \quad (171)$$

$$\mathcal{H}_1 = \frac{g_1}{2L} \sum_{q'kk'} b_{k+q'-2k_F}^\dagger a_{k'-q'+2k_F}^\dagger b_{k'} a_k + \frac{g_1}{2L} \sum_{q'kk'} a_{k+q'+2k_F}^\dagger b_{k'-q'-2k_F}^\dagger a_{k'} b_k. \quad (172)$$

In eq. (172), q' is a small momentum defined such that $q = q' \pm 2k_F$. The coupling constants should be taken as $g_2 \simeq g_4 \simeq V_0$, and $g_1 \simeq V_{2k_F}$. However, in the following we treat these three constants to be independent parameters. The momentum-transfer cut-off is introduced for the summation over q and q' . The Tomonaga-Luttinger model is defined by

$$\mathcal{H}_{\text{TL}} = \mathcal{H}_0 + \mathcal{H}_4 + \mathcal{H}_2. \quad (173)$$

Note that for the spin-less model there should be no distinction between \mathcal{H}_2 and \mathcal{H}_1 [33].

The interactions \mathcal{H}_4 and \mathcal{H}_2 can be expressed in terms of the density operators $\rho_1(p)$ and $\rho_2(p)$ defined by

$$\rho_1(p) = \sum_k \left[a_{k-p}^\dagger a_k - \delta_{p,0} \langle a_k^\dagger a_k \rangle_0 \right], \quad (174)$$

$$\rho_2(p) = \sum_k \left[b_{k-p}^\dagger b_k - \delta_{p,0} \langle b_k^\dagger b_k \rangle_0 \right]. \quad (175)$$

Here $\langle a_k^\dagger a_k \rangle_0 = \theta(k_F - k)$ and $\langle b_k^\dagger b_k \rangle_0 = \theta(k_F + k)$, and these terms are required to define the deviation from the noninteracting value without an ambiguity caused by the occupation of the negative energy states. Equations (170) and (171) can be rewritten in the following forms apart from a renormalization of the chemical potential that can be absorbed in to k_F ,

$$\mathcal{H}_4 = \frac{g_4}{L} \sum_{p>0} \rho_1(-p) \rho_1(p) + \frac{g_4}{L} \sum_{p>0} \rho_2(-p) \rho_2(p), \quad (176)$$

$$\mathcal{H}_2 = \frac{g_2}{L} \sum_{p>0} \rho_1(-p) \rho_2(p) + \frac{g_2}{L} \sum_{p>0} \rho_2(-p) \rho_1(p). \quad (177)$$

These two density operators satisfy the commutation relations

$$\left[\rho_1(p), \rho_1(-p') \right] = \frac{Lp}{2\pi} \delta_{pp'}, \quad \left[\rho_2(-p), \rho_2(p') \right] = \frac{Lp}{2\pi} \delta_{pp'}. \quad (178)$$

One notable feature is that these two commutation relations are equivalent to those of the bose operators,

$$C_p = \sqrt{\frac{2\pi}{Lp}} \rho_1(p), \quad C_p^\dagger = \sqrt{\frac{2\pi}{Lp}} \rho_1(-p), \quad (179)$$

$$C_{-p} = \sqrt{\frac{2\pi}{Lp}} \rho_2(-p), \quad C_{-p}^\dagger = \sqrt{\frac{2\pi}{Lp}} \rho_2(p), \quad (180)$$

$$[C_p, C_{p'}^\dagger] = \delta_{pp'}, \quad [C_{-p}, C_{-p'}^\dagger] = \delta_{pp'}, \quad (181)$$

where $p > 0$. The commutation relation of the density operators and Hamiltonian can be calculated by using eqs. (167) and (174)–(177) as

$$[\rho_1(p), \mathcal{H}_0] = v_F p \rho_1(p), \quad [\rho_2(-p), \mathcal{H}_0] = v_F p \rho_2(-p), \quad (182)$$

$$[\rho_1(p), \mathcal{H}_4] = \tilde{g}_4 v_F p \rho_1(p), \quad [\rho_2(-p), \mathcal{H}_4] = \tilde{g}_4 v_F p \rho_2(-p), \quad (183)$$

$$[\rho_1(p), \mathcal{H}_2] = \tilde{g}_2 v_F p \rho_2(p), \quad [\rho_2(-p), \mathcal{H}_2] = \tilde{g}_2 v_F p \rho_1(-p), \quad (184)$$

where $\tilde{g}_4 = g_4/(2\pi v_F)$, and $\tilde{g}_2 = g_2/(2\pi v_F)$.

5.2 Two conservation laws

The operator for the charge and current are defined by

$$\rho_c(p) = \rho_1(p) + \rho_2(p), \quad \rho_J(p) = \rho_1(p) - \rho_2(p). \quad (185)$$

In the real space, the operators for the left and right movers $\nu = 1, 2$ are written in the form

$$\rho_\nu(x) = \frac{1}{L} \sum_{p>0} \left(\rho_\nu(p) e^{ipx} + \rho_\nu(-p) e^{-ipx} \right). \quad (186)$$

The equation of motion for $\rho_c(x)$ and $\rho_J(x)$ are derived from the Heisenberg equation using the commutation relations in eqs. (182)–(184),

$$\frac{\partial}{\partial t} \rho_c(x, t) + v_J \frac{\partial}{\partial x} \rho_J(x, t) = 0, \quad v_J = v_F (1 + \tilde{g}_4 - \tilde{g}_2), \quad (187)$$

$$\frac{\partial}{\partial t} \rho_J(x, t) + v_N \frac{\partial}{\partial x} \rho_c(x, t) = 0, \quad v_N = v_F (1 + \tilde{g}_4 + \tilde{g}_2). \quad (188)$$

Because there are two independent equations for $\rho_c(x, t)$ and $\rho_J(x, t)$, the explicit form of these Heisenberg operators can be calculated analytically;

$$\left(\frac{\partial^2}{\partial t^2} - v_\rho^2 \frac{\partial^2}{\partial x^2} \right) \rho_c(x, t) = 0, \quad \left(\frac{\partial^2}{\partial t^2} - v_\rho^2 \frac{\partial^2}{\partial x^2} \right) \rho_J(x, t) = 0, \quad (189)$$

$$v_\rho^2 = v_J v_N. \quad (190)$$

The relation among the three velocities v_J , v_N and v_ρ can be summarized as

$$v_J = K_\rho v_\rho, \quad v_N = \frac{v_\rho}{K_\rho}, \quad K_\rho \equiv \sqrt{\frac{1 + \tilde{g}_4 - \tilde{g}_2}{1 + \tilde{g}_4 + \tilde{g}_2}}. \quad (191)$$

5.3 Charge and current correlation functions

Owing to the property shown in eq. (189), the correlation functions for the density operators

$$\chi_{\mu\nu}^r(p, t) = i \frac{1}{L} \theta(t) \langle [\rho_\mu(p, t), \rho_\nu(-p)] \rangle, \quad \text{for } \mu, \nu = 1, 2 \quad (192)$$

can also be calculated exactly. The equation of motion for these correlations are given by

$$\begin{aligned} i \frac{\partial}{\partial t} \chi_{\mu\nu}^r(p, t) &= -\frac{1}{L} \delta(t) \langle [\rho_\mu(p), \rho_\nu(-p)] \rangle - \theta(t) \frac{1}{L} \left\langle \left[\frac{\partial \rho_\mu(p, t)}{\partial t}, \rho_\nu(-p) \right] \right\rangle, \\ &= -\frac{p}{2\pi} \tau_{\mu\nu}^3 \delta(t) + i \theta(t) \frac{1}{L} \langle [\rho_\mu(p, t), \mathcal{H}_{\text{TL}}], \rho_\nu(-p) \rangle, \end{aligned} \quad (193)$$

where τ^3 is a Pauli matrix:

$$\tau^1 = \begin{bmatrix} 0 & 1 \\ 1 & 0 \end{bmatrix}, \quad \tau^2 = \begin{bmatrix} 0 & -i \\ i & 0 \end{bmatrix}, \quad \tau^3 = \begin{bmatrix} 1 & 0 \\ 0 & -1 \end{bmatrix}, \quad \mathbf{1} = \begin{bmatrix} 1 & 0 \\ 0 & 1 \end{bmatrix}. \quad (194)$$

The commutation relation $[\rho_\mu(p, t), \mathcal{H}_{\text{TL}}]$ in eq. (193) can be calculated by using eqs. (182)–(184). Then, by carrying out the Fourier transform with

respect to t , we obtain

$$\left\{ \omega \boldsymbol{\tau}^3 - v_\rho p \left(\cosh \varphi \mathbf{1} + \sinh \varphi \boldsymbol{\tau}^1 \right) \right\} \boldsymbol{\chi}^r(p, \omega) = -\frac{p}{2\pi} \mathbf{1}, \quad (195)$$

$$\cosh \varphi \equiv \frac{1 + \tilde{g}_4}{\sqrt{(1 + \tilde{g}_4)^2 - \tilde{g}_2^2}} = \frac{1}{2} \left(\frac{1}{K_\rho} + K_\rho \right), \quad (196)$$

$$\sinh \varphi \equiv \frac{\tilde{g}_2}{\sqrt{(1 + \tilde{g}_4)^2 - \tilde{g}_2^2}} = \frac{1}{2} \left(\frac{1}{K_\rho} - K_\rho \right). \quad (197)$$

Note that, $\cosh \varphi \mathbf{1} + \sinh \varphi \boldsymbol{\tau}^1 = \exp(\varphi \boldsymbol{\tau}^1)$. The Bogoliubov transformation given by $\exp(\varphi \boldsymbol{\tau}^1/2)$ has a property,

$$\boldsymbol{\tau}^3 = \exp\left(\frac{\varphi \boldsymbol{\tau}^1}{2}\right) \boldsymbol{\tau}^3 \exp\left(\frac{\varphi \boldsymbol{\tau}^1}{2}\right). \quad (198)$$

Therefore, eq. (195) can be diagonalized, as

$$\exp\left(\frac{\varphi \boldsymbol{\tau}^1}{2}\right) \left\{ \omega \boldsymbol{\tau}^3 - v_\rho p \mathbf{1} \right\} \exp\left(\frac{\varphi \boldsymbol{\tau}^1}{2}\right) \boldsymbol{\chi}^r(p, \omega) = -\frac{p}{2\pi} \mathbf{1}. \quad (199)$$

With this transformation by $\exp(\varphi \boldsymbol{\tau}^1/2)$, the operators C_p and C_{-p}^\dagger are transformed into

$$\begin{bmatrix} \gamma_p \\ \gamma_{-p}^\dagger \end{bmatrix} = \begin{bmatrix} \cosh(\varphi/2) & \sinh(\varphi/2) \\ \sinh(\varphi/2) & \cosh(\varphi/2) \end{bmatrix} \begin{bmatrix} C_p \\ C_{-p}^\dagger \end{bmatrix}, \quad (200)$$

$$\cosh(\varphi/2) = \frac{1}{2} \left(\frac{1}{\sqrt{K_\rho}} + \sqrt{K_\rho} \right), \quad \sinh(\varphi/2) = \frac{1}{2} \left(\frac{1}{\sqrt{K_\rho}} - \sqrt{K_\rho} \right), \quad (201)$$

where the bose statistics is preserved for the new operators, $[\gamma_p, \gamma_{p'}^\dagger] = \delta_{pp'}$. The explicit form of $\boldsymbol{\chi}^r(p, \omega)$ is determined by eq. (199),

$$\boldsymbol{\chi}^r(p, \omega) = -\frac{p}{2\pi} \exp\left(-\frac{\varphi \boldsymbol{\tau}^1}{2}\right) \left\{ D_+^r(p, \omega) \boldsymbol{\tau}^3 + D_-^r(p, \omega) \mathbf{1} \right\} \exp\left(-\frac{\varphi \boldsymbol{\tau}^1}{2}\right)$$

$$= -\frac{p}{2\pi} \left\{ D_+^r(p, \omega) \boldsymbol{\tau}^3 + D_-^r(p, \omega) (\cosh \varphi \mathbf{1} - \sinh \varphi \boldsymbol{\tau}^1) \right\}, \quad (202)$$

$$D_{\pm}^r(p, \omega) = \frac{1}{2} \left(\frac{1}{\omega - v_{\rho} p + i\delta} \pm \frac{1}{\omega + v_{\rho} p + i\delta} \right). \quad (203)$$

The charge susceptibility $\chi_c^r(p, \omega)$, which corresponds to the ρ_c - ρ_c correlation function, is given by

$$\chi_c^r(p, \omega) = \sum_{\mu\nu} \chi_{\mu\nu}^r(p, \omega) = -\frac{K_{\rho}}{\pi v_{\rho}} \frac{(v_{\rho} p)^2}{(\omega + i\delta)^2 - (v_{\rho} p)^2}. \quad (204)$$

Then, the uniform charge susceptibility is given by $\lim_{p \rightarrow 0} \chi_c^r(p, 0) = K_{\rho}/(\pi v_{\rho})$. It becomes twice as large for the spin 1/2 fermions.

The current operator is determined by eqs. (185)–(187) as

$$J = e v_J \rho_J. \quad (205)$$

Therefore, the J - J correlation function is given by

$$K^r(p, \omega) = -\frac{e^2 K_{\rho} v_{\rho}}{\pi} \frac{(v_{\rho} p)^2}{(\omega + i\delta)^2 - (v_{\rho} p)^2}. \quad (206)$$

Then, the conductivity can be calculated with the Kubo formula,

$$\begin{aligned} \sigma(p, \omega) &= \frac{K^r(p, \omega) - K^r(p, 0)}{i\omega} \\ &= \frac{e^2 K_{\rho} v_{\rho}}{\pi} \frac{i\omega}{(\omega + i\delta)^2 - (v_{\rho} p)^2}. \end{aligned} \quad (207)$$

The conductivity $\sigma(p, \omega)$ for a uniform $p = 0$ and stationary $\omega = 0$ field depends on the order of taking the limits of $p \rightarrow 0$ and $\omega \rightarrow 0$. The Drude weight corresponds to the $p \rightarrow 0$ limit,

$$\text{Re } \sigma(0, \omega) = e^2 K_{\rho} v_{\rho} \delta(\omega), \quad (208)$$

In the real space, the conductivity takes the form

$$\sigma(x, \omega) = \int_{-\infty}^{\infty} \frac{dp}{2\pi} \sigma(p, \omega) e^{ipx}$$

$$\begin{aligned}
&= \int_{-\infty}^{\infty} \frac{dp}{2\pi} \frac{i e^2 K_\rho v_\rho}{2\pi} \left[\frac{1}{\omega - v_\rho p + i\delta} + \frac{1}{\omega + v_\rho p + i\delta} \right] e^{ipx} \\
&= \frac{e^2 K_\rho}{2\pi} e^{i \frac{\omega}{v_\rho} |x|} .
\end{aligned} \tag{209}$$

The dc conductance corresponds to the $\omega \rightarrow 0$ limit,

$$\sigma(x, 0) = \frac{e^2}{2\pi\hbar} K_\rho = \frac{e^2}{h} K_\rho , \tag{210}$$

where \hbar has been reinserted.

5.4 Boson representation of the Hamiltonian

We have seen in the above that the bosonic excitations play an important role on the transport properties of the Tomonaga-Luttinger model. Correspondingly, there is one notable feature in the commutation relations for the density operators in eqs. (182) and (183): the two parts of the Hamiltonian \mathcal{H}_0 and $\mathcal{H}_4/\tilde{g}_4$ show the same commutation relations. Therefore, one can introduce an effective Hamiltonian $\tilde{\mathcal{H}}_0$ defined by

$$\tilde{\mathcal{H}}_0 = \frac{2\pi v_F}{L} \sum_{p>0} \rho_1(-p) \rho_1(p) + \frac{2\pi v_F}{L} \sum_{p>0} \rho_2(-p) \rho_2(p) , \tag{211}$$

which reproduces the commutation relation eq. (182). Thus, the correlation functions can be calculated exactly by using $\tilde{\mathcal{H}}_0$ as a replacement for \mathcal{H}_0 . The effective Hamiltonian is written in a bilinear form with the boson operators,

$$\begin{aligned}
\tilde{\mathcal{H}}_{\text{TL}} &\equiv \tilde{\mathcal{H}}_0 + \mathcal{H}_4 + \mathcal{H}_2 \\
&= \sum_{p>0} \begin{bmatrix} C_p^\dagger & C_{-p} \end{bmatrix} v_\rho p \left(\cosh \varphi \mathbf{1} + \sinh \varphi \boldsymbol{\tau}^1 \right) \begin{bmatrix} C_p \\ C_{-p}^\dagger \end{bmatrix} \\
&= \sum_{p>0} v_\rho p \left(\gamma_p^\dagger \gamma_p + \gamma_{-p}^\dagger \gamma_{-p} \right) + \text{const} .
\end{aligned} \tag{212}$$

In this section, we have discussed only the two-particle correlation functions. The equation of motion for the single-particle Green's function can also be written in a closed form [34, 35], and the precise calculations have been reported in Refs. [36, 37]. Furthermore, for comprehensive description of the bosonization, see Ref. [38].

References

- [1] L. V. Keldysh: Sov. Phys. JETP **20**, 1018 (1965).
- [2] J. Schwinger: J. Math. Phys. **2**, 407 (1961).
- [3] L. P. Kadanoff and G. Baym: *Quantum Statistical Mechanics* (Benjamin, New York, 1962).
- [4] C. Caroli, R. Combescot, P. Nozieres, and D. Saint-James: J. Phys. C **4**, 916 (1971).
- [5] E. M. Lifshitz and L. P. Pitaevskii, *Physical Kinetics* (Pergamon, Oxford, 1981).
- [6] G. D. Mahan: *Many-Particle Physics* (Plenum Press, New York, 1990).
- [7] K. Cho, Z. Su, B. Hao, and L. Yu: Physics Reports **118**, Nos. 1&2, 1 (1985).
- [8] S. Datta, *Electronic transport in mesoscopic systems* (Cambridge University Press, Cambridge, 1997).
- [9] H. Haug and A. P. Jauho, *Quantum kinetics in transport and optics of semiconductors* (springer, Heidelberg, 1996).
- [10] P. Nozières, J. Low Temp. Phys. **17**, 31 (1974).
- [11] K. Yamada: Prog. Theor. Phys. **53**, 970 (1975); Prog. Theor. Phys. **54**, 316 (1975).
- [12] A. C. Hewson: *The Kondo Problem to Heavy Fermions* (Cambridge University Press, Cambridge, 1993).
- [13] A. L. Fetter and J. D. Walecka: *Quantum Theory of Many-Particle Systems* (McGRAW-HILL, New York, 1971).
- [14] S. Hersfield, J. H. Davies, and J. W. Wilkins: Phys. Rev. B **46** 7046, (1992).
- [15] Y. Meir and N. S. Wingreen: Phys. Rev. Lett. **68** 2512, (1992).
- [16] R. Landauer: Philos. Mag. **21** 863, (1970).

- [17] M. Büttiker, Y. Imry, R. Landauer and S. Pinhas: Phys. Rev. B **31** 6207, (1985).
- [18] D. S. Fisher and P. A. Lee: Phys. Rev. B **23** 6851, (1981); P. A. Lee and D. S. Fisher: Phys. Rev. Lett. **47**, 882 (1981).
- [19] A. Oguri: J. Phys. Soc. Jpn. **70** 2666, (2001); J. Phys. Soc. Jpn. **72** 3301, (2003).
- [20] J. W. Negele and H. Orland: *Quantum Many-Particle Systems* (Addison-Wesley, Redwood City, 1987).
- [21] A. Oguri: Phys. Rev. B **64**, 153305 (2001); J. Phys. Soc. Jpn. **74**, 110 (2005).
- [22] G. M. Éliashberg: Soviet Phys. JETP **14**, 886 (1962).
- [23] A. A. Abrikosov, L. P. Gor'kov, and I. Y. Dzyaloshinskii: *Quantum Field Theoretical Methods in Statistical Physics* (Pergamon, London, 1965).
- [24] A. Oguri: J. Phys. Soc. Jpn. **66**, 1427 (1997).
- [25] A. Oguri: Phys. Rev. B **56**, 13422 (1997); [Errata: **58**, 1690 (1998)].
- [26] A. Oguri: Phys. Rev. B **59**, 12240 (1999).
- [27] A. Oguri: Phys. Rev. B **63**, 115305 (2001); *ibid.* [Errata: **63**, 249901 (2001)].
- [28] J. S. Langer and V. Ambegaokar: Phys. Rev. **121**, 1090 (1961).
- [29] J. R. Schrieffer: *Theory of Superconductivity* (Benjamin, Reading, Massachusetts, 1964).
- [30] A. Oguri and A. C. Hewson: J. Phys. Soc. Jpn. **74**, 988 (2005).
- [31] A. Oguri, Y. Nisikawa and A. C. Hewson: J. Phys. Soc. Jpn. **74**, 2554 (2005).
- [32] Y. Nisikawa and A. Oguri, Phys. Rev. B **73**, 125108 (2006).
- [33] J. Sólyom, Adv. Phys. **28**, 201 (1979).

- [34] Y. Dzyaloshinskii, and A. I. Larkin: Soviet Phys. JETP **38**, 202 (1974).
- [35] E. U. Everts and H. Shultz: Solid State Commun. **15**, 1413 (1974).
- [36] J. Voit: Phys. Rev. B **47**, 6740 (1993).
- [37] V. Meden, and K. Schönhammer: Phys. Rev. B **46**, 15753 (1992).
- [38] F. D. M. Haldane, J. Phys. C **14**, 2585 (1981).